Remote Sensing of Environment 215 (2018) 452–470

Contents lists available at ScienceDirect

Remote Sensing of Environment

journal homepage: www.elsevier.com/locate/rse

Capability of Sentinel-2 data for estimating maximum evapotranspiration and irrigation requirements for tomato crop in Central Italy

Silvia Vanino[a], Pasquale Nino[a,*], Carlo De Michele[b], Salvatore Falanga Bolognesi[b], Guido D'Urso[c], Claudia Di Bene[d], Bruno Pennelli[d], Francesco Vuolo[e], Roberta Farina[d], Giuseppe Pulighe[a], Rosario Napoli[d]

[a] CREA Research Centre for Agricultural Policies and Bioeconomy, Via Po 14, Rome, Italy
[b] ARIESPACE s.r.l., Centro Direzionale IS. A3, 80143 Naples, Italy
[c] Department of Agricultural Sciences, University of Naples Federico II, Via Università 100, I-80055 Portici, Italy
[d] CREA Research Centre for Agriculture and Environment, Via della Navicella 2-4, Rome, Italy
[e] Institute of Surveying, Remote Sensing and Land Information, BOKU University, Peter-Jordan-Straße 82, 1190 Wien, Austria

ARTICLE INFO

Keywords:
Sentinel-2A
Evapotranspiration in standard condition
LAI
EPIC model
Irrigation requirements
Tomato
Multispectral

ABSTRACT

The occurrence of water shortages ascribed to projected climate change, especially in the Mediterranean region, fosters the interest in remote sensing (RS) applications to optimize water use in agriculture. Remote sensing evapotranspiration and water demand estimation over large cultivated areas were used to manage irrigation to minimize losses during the crop growing cycle. The research aimed to explore the potential of the MultiSpectral Instrument (MSI) sensor on board Sentinel-2A to estimate crop parameters, mainly surface albedo (α) and Leaf Area Index (LAI) that influence the dynamics of potential evapotranspiration (ET_p) and Irrigation Water Requirements (IWR) of processing tomato crop (*Solanum lycopersicum* L.). Maximum tomato ET_p was calculated according to the FAO Penman-Monteith equation (FAO-56 PM) using appropriate values of canopy parameters derived by processing Sentinel-2A data in combination with daily weather information. For comparison, we used the actual crop evapotranspiration (ET_a) derived from the soil water balance (SWB) module in the Environmental Policy Integrated Climate (EPIC) model and calibrated with in-situ Root Zone Soil Moisture (RZSM). The experiment was set up in a privately-owned farm located in the Tarquinia irrigation district (Central Italy) during two growing seasons, within the framework of the EU Project FATIMA (FArming Tools for external nutrient Inputs and water Management). The results showed that canopy growth, maximum evapotranspiration (ET_p) and IWR were accurately inferred from satellite observations following seasonal rainfall and air temperature patterns. The net estimated IWR from satellite observations for the two-growing seasons was about 272 and 338 mm in 2016 and 2017, respectively. Such estimated requirement was lower compared with the actual amount supplied by the farmer with sprinkler and drip micro-irrigation system in both growing seasons resulting in 364 (276 mm drip micro-irrigation, and 88 mm sprinkler) and 662 (574 mm drip micro-irrigation, and 88 mm sprinkler) mm, respectively. Our findings indicated the suitability of Sentinel-2A to predict tomato water demand at field level, providing useful information for optimizing the irrigation over extended farmland.

1. Introduction

Evidence suggests that human-induced greenhouse gases emissions have altered our climate at a relatively rapid rate (Allen et al., 2009; IPCC, 2013), with the consequence that rising global temperatures and changes in precipitation pattern drastically exposed water-limited environments and agriculture, restricting crop yield, production and food availability (Avramova et al., 2016; McKersie, 2015; Moore and Lobell, 2014). Freshwater scarcity is widely acknowledged as a global systemic risk in terms of potential impact (Mekonnen and Hoekstra, 2016), especially in agricultural production, which uses about 70% of total freshwater withdrawals (WWAP, 2015). In particular, the impacts of climate change on European (EU) agriculture may increase productivity in northern latitudes, while in southern latitude projection indicated reduction in rainfall, and water availability, problems with salinization and increase in pest and disease outbreaks (Falloon and Betts, 2010; Kaley et al., 2017).

All above considered, there is an urgent need to seek out

* Corresponding author.
E-mail address: pasquale.nino@crea.gov.it (P. Nino).

https://doi.org/10.1016/j.rse.2018.06.035
Received 14 October 2017; Received in revised form 13 June 2018; Accepted 24 June 2018
Available online 03 July 2018

technological advancements and scalable solutions in the context of Precision Farming (PF) (Lal and Stewart, 2016; Liaghat and Balasundram, 2010; Moran et al., 1997; Mulla, 2013; Vuolo et al., 2015; Zarco-Tejada et al., 2014) to address management strategies on water inputs in response to seasonal drought.

This objective requires timely and reliable estimation of crop evapotranspiration (ET) and Irrigation Water Requirements (IWR) at field level with high spatial and temporal resolution. Soil water balance (SWB) models present limitations when applied to wide areas due to complexity of input data required, with special concern to soil hydraulic properties, interaction with groundwater, variability of plant development due to different crop varieties and management practices. Diversely, Earth Observation (EO) techniques provide reliable and suitable data to feed PF applications and serve several end-users (i.e. farmers, landowners and decision makers). High temporal and spatial resolution multi-spectral imagery can be used to manage irrigation scheduling based on near real-time actual crop needs (Calera et al., 2017). One advantage is the detection of the actual crop development which influences the entity of evapotranspiration fluxes and hence the irrigation requirements. Although extensive research has been carried out on ET crop estimation for water management using EO data, to date one of the major limitation for their applicability and technological transfer was the limited spatial and temporal resolution of the sensors (Bisquert et al., 2016). In this context, the recent advent of Sentinel-2 mission from European Space Agency (ESA), as part of the programme Copernicus (http://www.copernicus.eu/) (Drusch et al., 2012), has greatly enhanced the possibilities for a routine monitoring of crop parameters, such as LAI. The Multi Spectral Instrument (MSI) on board of Sentinel-2 captures data at 10, 20 and 60-meter spatial resolution over 13 spectral bands and with a very high temporal resolution of five days at the equator. Thanks to the rich information content the application of inversion techniques of radiative transfer models is now possible, providing robust physical basis for describing crop reflectance and estimating crop parameters such as LAI (Herrmann et al., 2011; Laurent et al., 2014; Richter et al., 2012; Verrelst et al., 2015). The combination of freely available satellite imagery, high resolution, novel spectral capabilities, a swath width of 290 km and frequent revisit times is stimulating the development of operational and commercial uses of EO data tailored for PF applications, as well as for scientific projects. The Sentinel-2 mission also provides data to be integrated in a tool for improving the quality of existing Web-GIS Satellite-based Irrigation Advisory Services - IAS (Calera et al., 2017; Richter et al., 2012; Vuolo et al., 2015; D'Urso et al., 2008) or other similar implementations foreseen in the near future (Pereira, 2017).

This study focuses on the determination of the Irrigation Water Requirements in tomato crops by means of Copernicus Sentinel-2A data. It uses Environmental Policy Integrated Climate (EPIC) crop growth model simulations for the comparison of the predicted crop evapotranspiration. The work was developed in the context of the FATIMA project (http://fatima-h2020.eu/), financed by the EU Commission under the HORIZON 2020 programme to develop and adopt innovative farming tools and service capacities that help the intensive farm sector to optimize its external input management (nutrients, energy and water) and productivity. The results of this research can be used for developing operational tools for monitoring water use trends of irrigated crop at commercial farm level in a Mediterranean environment in Central Italy.

2. Methodological approach to estimate potential evapotranspiration from Earth Observation

Over the past two decades, the improvements in the technical capabilities of spaceborne EO sensors allowed different approach for implementing potential evapotranspiration (ET_p) estimation from satellite imagery. Several reviews have attempted to evaluate ET_p EO-based methods and their performances, with special focus on irrigation management in agriculture, considering scales and temporal evolution during the growing season (Allen et al., 2011; Calera et al., 2017; D'Urso, 2010). To date, according to those reviews, two main groups of EO-based methods for ET estimation can be distinguished. The first group considers observations in the thermal range to estimate latent heat flux as a residual of surface energy balance, hence the actual evapotranspiration ET_a, accordingly to different schematizations (Allen et al., 2007; Bastiaanssen et al., 1998; Kalma et al., 2008; Kustas et al., 2016). Surface energy balance methods can detect crop water stress but suffer from the technical limitations of thermal observations from space in terms of spatial and temporal resolution. The second group contemplates visible (VIS) and near-infrared (NIR) wavelengths for characterizing the crop development in the application of the FAO-56 Penman–Monteith (FAO-56 PM) model (Allen et al., 1998); in this case, it is generally assumed that the crop is in "*standard conditions*", i.e. in a disease-free environment with adequate fertilization and sufficient soil water availability (irrigation applied). Often this value of evapotranspiration is referred to as "potential", which might introduce some confusion with the term "reference", for this reason, we prefer to use in this text the complete definition of FAO-56 PM, i.e. evapotranspiration in standard conditions ET_p, which means maximum value of crop evapotranspiration. Thus, we derive the maximum IWR for a crop at a given development stage. Under the hypothesis of a uniform soil cover, the Penman-Monteith approach derives surface resistances to heat and vapour transfer to the atmosphere by using vegetation parameters, namely Leaf Area Index (LAI – key parameter characterizing the structure and functioning of vegetation cover, that influence crop productivity), surface albedo (α-influences the net radiation of the surface, which is the primary source of the energy exchange for the evaporation process), and crop height (h_c - influences the aerodynamic resistance term of the FAO-56 Penman-Monteith equation and the turbulent transfer of vapour from the crop into the atmosphere) (Allen et al., 1998; D'Urso, 2001). Since for a crop in standard conditions, a minimum value of stomatal resistance can be considered for most herbaceous crops ($\approx 100\ sm^{-1}$), the surface resistance became a function of LAI only. This is also referred in the FAO-56 paper as the "one-step" or "direct" approach. During recent years, there has been a consistent effort to estimate vegetation parameters (α-LAI) from EO in the VIS and NIR regions (Atzberger and Richter, 2012; Vuolo et al., 2015), allowing to adapt the Penman–Monteith equation to be used directly with EO based LAI and α value (D'Urso, 2010), which can be measured in the field for providing an assessment of accuracy of the ET method, in addition to the below mentioned micro-meteorological techniques, and to derive the maximum IWR. The use of EO-based "one-step" FAO-56 PM method has become more popular recently for assessing ET_p under different hydro-climatic regions and crops such as wheat, cotton, corn, grapes and orchards (Farg et al., 2012; Glenn et al., 2011; Vanino et al., 2015). This approach has the advantage of being easily implemented, especially over homogeneous landscapes represented by irrigated farmland under unstressed conditions (Anderson et al., 2012).

Another category of EO methods for estimating ET_p is based on the traditional concept of the so-called crop coefficient (K_c), defined as the ratio of the unstressed crop evapotranspiration to the reference evapotranspiration (ET_0). K_c is specific to each crop and reflects the canopy development due to agronomic practices (including irrigation) over the course of the growing season. Hence, in this "two-steps" approach, ET_p is estimated as the product of the reference evapotranspiration (ET_0, depending only from atmospheric conditions) and the K_c. Several studies have demonstrated the linear relationship between K_c and different Vegetation Index (VIs), such as the Normalized Difference Vegetation Index (NDVI, Tucker et al., 1979) or the Soil Adjusted Vegetation Index (SAVI, Huete, 1988), derived from spectral observations in the VIS and NIR region (D'Urso and Calera, 2006; Neale et al., 1989). However, the determination of the empirical parameters of the relationship between K_c and VIs would requires measurements of ET over well irrigated crops, by using micro-meteorological methods such as lysimeters,

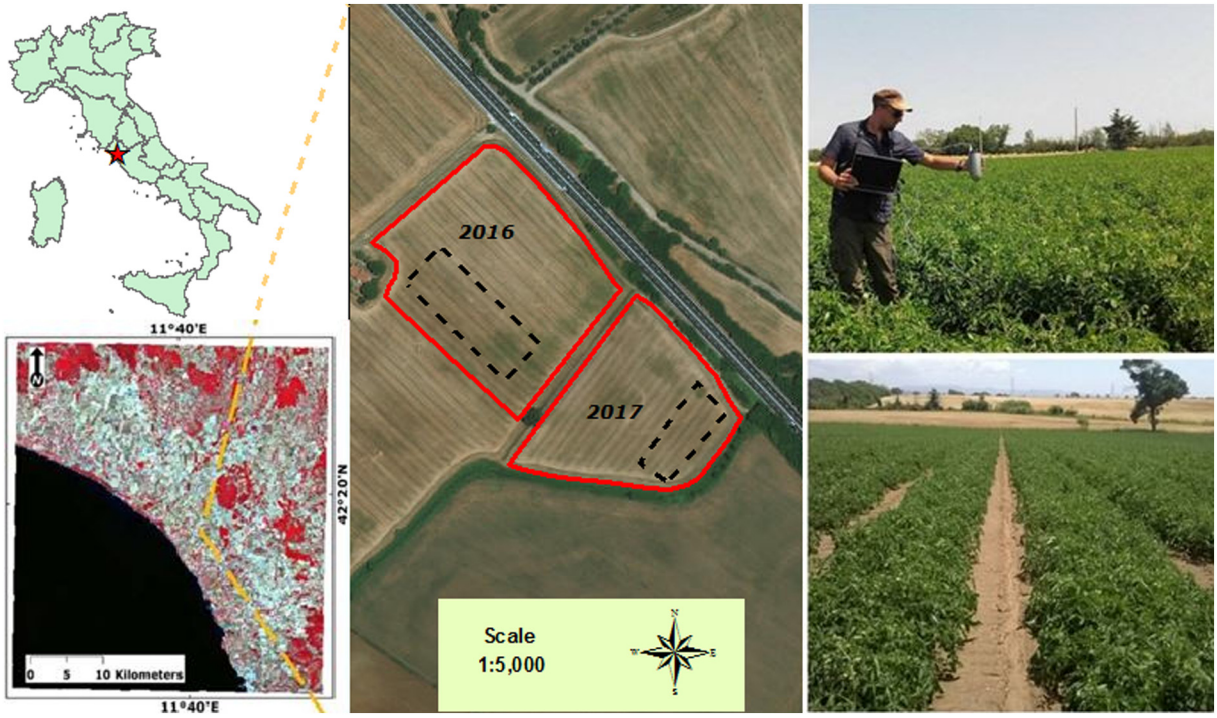

Fig. 1. Study area location and experimental field plots within the privately-owned farm in Tarquinia Municipality coastal plain (western Central Italy).

Bowen Ratio, and Eddy Covariance. This calibration procedure is seldom applied, leaving the definition of K_c (VIs) to visual field inspections of crop growth and phenology, which are subjective and qualitative.

3. Materials and methods

3.1. Study area

The study area is in the Nitrate Vulnerable Zone (NVZ) of Tarquinia Municipality coastal plain (Viterbo Province, Lazio Region; 7 km NW of Tarquinia, 2.7 km from seashore - 42° 69′ N and 11° 69′ E, at an average altitude of 25 m above sea level, with 3% mean slope) and it is part of the Water User Association (WUA) district of "Maremma Etrusca", one of the largest agricultural irrigation districts of Western Central Italy. The WUA manages the agricultural irrigation infrastructural network in a supply mode using river and artificial channel waters (Fig. 1). The area is characterized by intensive agricultural management due to the production of irrigated crops (mostly processing tomato) and the large use of mineral N fertilizer, causing groundwater pollution. Therefore, it was selected as the Italian pilot case study for the FATIMA project to:

- Establish innovative and new farm tools and service capacities that help the intensive farm sector.
- Optimize productivity and external management inputs (water, nutrients and energy).

The area is on Pleistocene medium and low marine terraces (Quaternary period), during the Pleistocene epoch, and on recent local lowlands with limited costal aquifers salt-water intrusion. The climate is typical Mediterranean (Koppen classification: Csa) characterized by warm dry summers, mild winters, and with an average annual rainfall of approximately 600 mm, mainly concentrated in autumn and spring. The mean daily temperature is 15.3 °C (ranging from 7.7 °C in January and of 23.7 °C in July).

3.2. Experimental field plots description

The experimental campaign was carried out during the 2016 and 2017 growing seasons within a 20 ha privately owned farm, with a crop rotation of durum wheat (*Triticum durum* Desf. var. Iride) and processing tomato (*Solanum lycopersicum* L. var. Vulcano) (Fig. 1). The soil present a clay loam texture, and is classified as *Calcaric Cambic Phaeozems* according to FAO system (IUSS-WRB, 2015).

Tomato plants (variety "Vulcano") were transplanted at four-leaves stage 5th May 2016 and 29th April 2017, in an experimental area of about 3 ha with a plant density of 2.9 plants m^{-2}. The tomato variety selected was suitable for mechanized harvesting which requires determinate or bush-like growth (max 0.4–0.6 m), resistance to overripe and contemporaneity of fruit ripe. Irrigation was provided by a sprinkler system in the first three weeks after transplanting and by micro-irrigation (combined by fertilization) during the rest of the growing season. Irrigation scheduling was established by the farmer based on his own practical experience.

During the 2016 and 2017 growing seasons the total rainfall was 75 and 18 mm. The irrigation water applied by micro-irrigation was recorded through a flanged - cast iron water flow meter (Bontempi DN065), resulting in a total amount of 276 and 574 mm/ha for 2016 and 2017 respectively. Pest and weeds control was performed according to the current farming management practice. The crop was harvested on 18th August 2016 (90.7 ton/ha yield) and on 8th August 2017 (72.3 ton/ha yield), when ripe fruit rate reached about 90%, with an average crop cycle length of around 106 days.

3.3. Data set and processing procedure

The data set and the processing procedure to estimate ET_p and IWR are summarized in Fig. 2.

This included daily meteorological information, EO data from Sentinel-2A satellite, in-situ crop parameters and soil water content measurements, records of irrigation applied. The flowchart highlighted that field measures were used both to validate EO maps and to calibrate EPIC model. In details, canopy reflectance and LAI measures were used

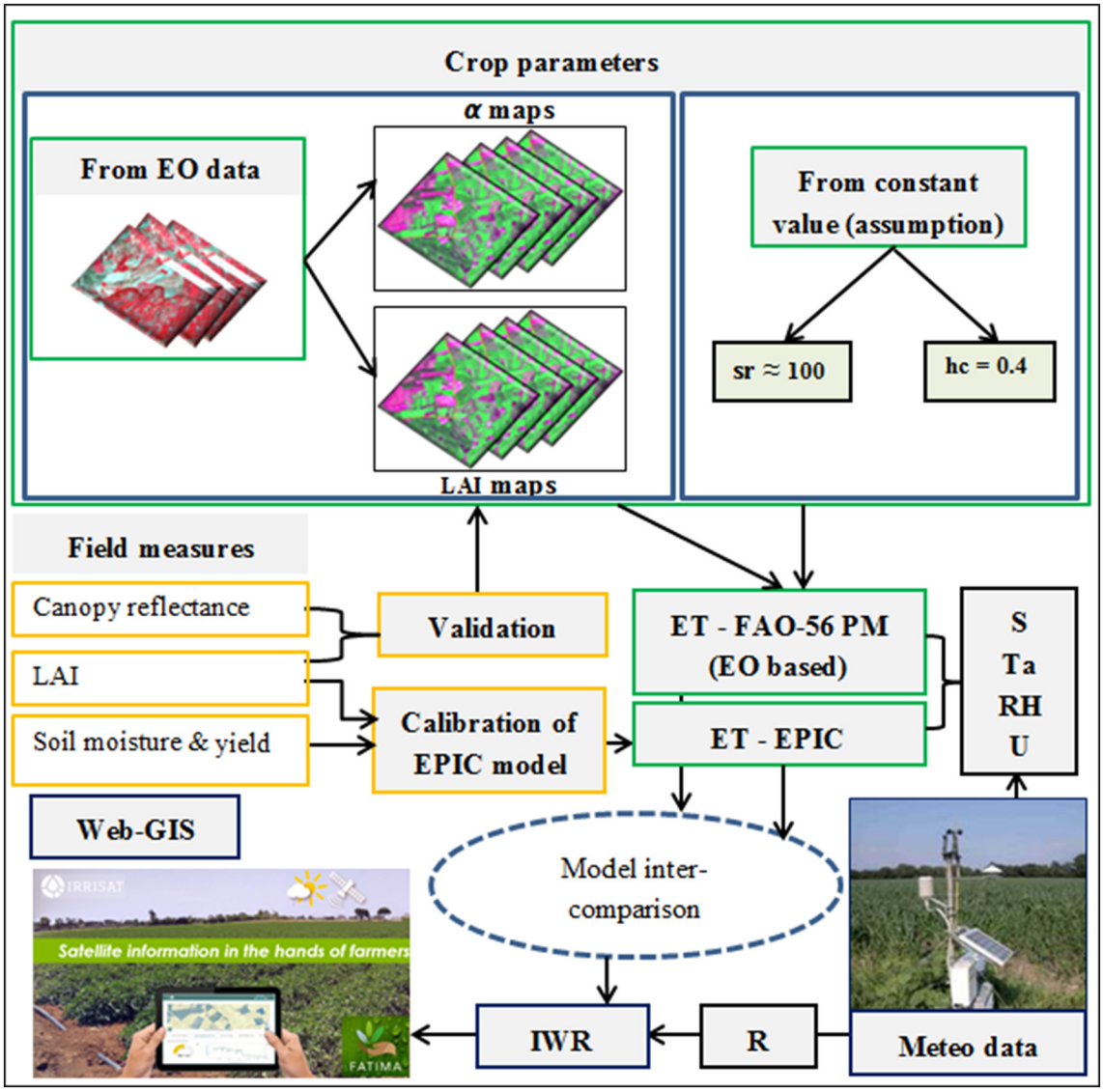

Fig. 2. Flowchart showing data sets and processing procedure required to estimate crop potential evapotranspiration (ET_p), and Irrigation Water Requirements (IWR), EO-based direct FAO-56 PM method. Where, sr: minimum stomatal resistance (sm^{-1}), h_c: crop height (m), S: Solar radiation (Wm^{-2}), Ta: Air temperature (°C), RH: Air humidity (%), U: Wind speed (ms^{-1}), R: Rainfall (mm).

to validate α and LAI maps, while LAI, soil moisture and tomato yield were used to EPIC model calibration. After EO maps validation and model calibration, ET was estimated by EO-based direct FAO-56 PM method and EPIC model. Both ET results were compared using performance statistical indicators as detailed in Section 3.4.3.

3.3.1. Meteorological data

Daily meteorological data (from 2004 to present) include solar radiation (S - Wm^{-2}), air temperature (T_a - °C), air humidity (RH - %), wind speed (U - ms^{-1}) and rainfall (R - mm). They were measured at the Agrometeorological Service station of Lazio Region (ARSIAL) located in the Tarquinia Municipality (Central Italy). This data were used to compute FAO-56 PM reference evapotranspiration (ET_0) and the IWR for 2016 and 2017.

Table 1 shows the weather conditions in 2016 and 2017. In the period January to August, the two years presented similar mean temperature, i.e. 17.3 °C (2016) and 17.1 °C (2017). This was higher than the long-term (2004–2017) average of 16.1 °C. Conversely, rainfall, from January to August, was extremely different for the two years, 260 vs 120 mm in 2016 and 2017, respectively. As for temperature, both years showed a deviation respect to the rainfall long-term average of −92 mm in 2016 and −232 mm in 2017.

Table 1
Monthly (January–August) mean temperature (°C) and rainfall (mm) during the 2016 and 2017 growing seasons in comparison with the long-term (2004–2017) average at Agrometeorological Service station of Lazio Region (ARSIAL) - in Tarquinia Municipality (western Central Italy).

	Jan	Feb	Mar	Apr	May	Jun	Jul	Aug
Temperature 2016 (°C)	9.8	11.8	11.9	15.7	18.0	22.3	24.6	24.5
Temperature 2017 (°C)	7.1	10.9	12.1	13.9	18.5	23.4	24.9	25.5
Temperature long-term average	8.8	8.1	11.2	14.3	17.0	21.3	23.6	24.4
Rainfall 2016 (mm)	36.6	99.2	34.0	10.2	34.8	41.6	3.2	0.4
Rainfall 2017 (mm)	16.2	43.9	17.5	23.4	6.7	11.0	0.0	0.9
Rainfall long-term average	75.4	58.4	71.8	38.2	31.0	21.5	45.5	9.9

Seasonal variation in ET_0 is shown in Fig. 3 for 2016 and 2017. Cumulative ET_0 during the two growing seasons was 513 mm (from 3rd May to 18th of August 2016) and 516 mm (from 29th April to 8th of August 2017). In 2016 growing season the average daily ET_0 was 4.73 mm d^{-1}, ranging from 2.13 mm d^{-1} (11th May) to 7.69 mm d^{-1}

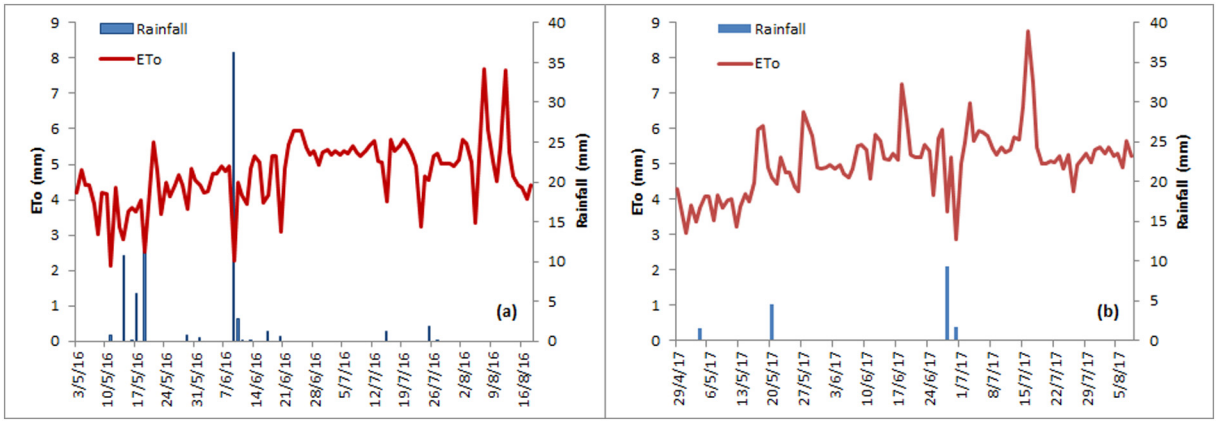

Fig. 3. Reference evapotranspiration (FAO-56 PM ET_0, in mm d^{-1}) and rainfall events mm d^{-1} for the growing season 2016 (a) and 2017 (b) for the experimental field.

Table 2
Sentinel-2 dataset: central wavelength, bandwidth, and spatial resolution for the 13 spectral bands of the MSI. Purpose of each band is also shown.

Band	Center λ	Spectral width Δλ	Spatial resolution	Purpose
#	nm	nm	m	
B1	443	20	60	Atmospheric correction (aerosol scattering)
B2	490	65	10	Sensitive to vegetation senescing, carotenoid, browning and soil background; atmospheric correction (aerosol scattering)
B3	560	35	10	Green peak, sensitive to total chlorophyll in vegetation
B4	665	30	10	Maximum chlorophyll absorption
B5	705	15	20	Position of red edge; consolidation of atmospheric corrections/flourescence baseline.
B6	740	15	20	Position of red edge, atmospheric correction, retrieval of aerosol load.
B7	783	20	20	Leaf Area Index (LAI), edge of the Near-Infrared (NIR) plateau.
B8	842	115	10	LAI
B8a	865	20	20	NIR plateau, sensitive to total chlorophyll, biomass, LAI and protein; water vapour absorption reference; retrieval of aerosol load and type.
B9	945	20	60	Water vapour absorption, atmospheric correction.
B10	1375	30	60	Detection of thin cirrus for atmospheric correction.
B11	1610	90	20	Sensitive to lignin, starch and forest above ground biomass. Snow/ice/cloud separation.
B12	2190	180	20	Assessment of Mediterranean vegetation conditions. Distinction of clay soils for the monitoring of soil erosion. Distinction between live biomass, dead biomass and soil, e.g. for burn scars mapping.

Note: The nine bands used for LAI estimation are highlighted in bold, while for bands used in the α calculation see Table 3.

Table 3
Weighting coefficients for the calculation of albedo by using Eq. (1).

Band	Center λ	Spectral width Δλ	Esun	ω_{bi}
Number	(μm)	(μm)	(W m^{-2})	(−)
1	0.443	0.020	1893	
2	0.490	0.065	1927	0.1324
3	0.560	0.035	1846	0.1269
4	0.665	0.030	1528	0.1051
5	0.705	0.015	1413	0.0971
6	0.740	0.015	1294	0.0890
7	0.783	0.020	1190	0.0818
8	0.842	0.115	1050	0.0722
8a	0.865	0.020	970	
9	0.945	0.020	831	
10	1.375	0.030	360	
11	1.610	0.090	242	0.0167
12	2.190	0.180	3	0.0002

(7^{th} August), while in 2017 the average daily ET_0 was 5.06 mm d^{-1}, ranging from 2.87 mm d^{-1} (30^{th} June) to 8.77 mm d^{-1} (16^{th} July).

3.3.2. Earth Observation products

We have used EO data acquired from the Copernicus Sentinel-2 satellite. The Sentinel-2 mission is based on a constellation of two identical satellites (Sentinel-2A, launched on 23^{rd} June 2015, and Sentinel-2B, launched on 7^{th} March 2017) both orbiting at an altitude of 786 km, 180° apart for optimal coverage and data delivery. Together they cover all Earth's land surfaces, large islands, inland and coastal waters every five days at the equator (http://www.esa.int/Our_Activities/Observing_the_Earth/Copernicus/Sentinel-2), ESA delivers Level 1C orthorectified Top of Atmosphere (TOA) reflectance through the Copernicus Open Access Hub (https://scihub.copernicus.eu/

Table 4
Temporal frequency of the Sentinel-2A cloud free images available for the field experimental trial, during the 2016 and 2017 growing seasons. Date in bold refers to the day when field vegetation measures were done.

Year	DOY	Date	Year	DOY	Date
2016	130	9/5	2017	131	11/5
	160	**8/6**		151	31/5
	165	15/6		154	**3/6**
	177	**25/6**		164	13/6
	190	**8/7**		174	**23/6**
	200	18/7		184	5/7
	217	4/8		194	**13/7**
	220	7/8		204	23/7
				214	**2/8**
				221	7/8

DOY – Day of the year.

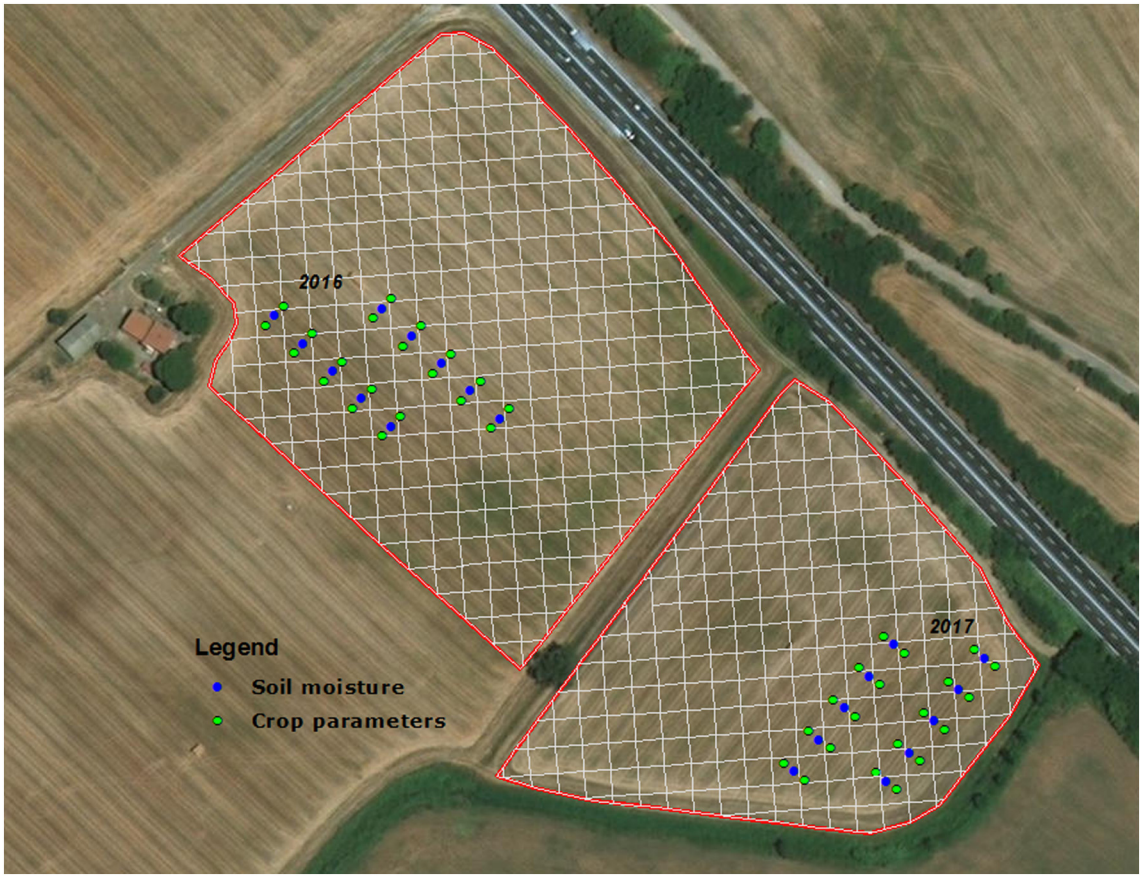

Fig. 4. Layout of experimental field. Blue dot represents the soil moisture measurements point, while green dot represents crop parameters (LAI, spectral reflectance and chlorophyll content) measurements point. Sentinel-2A grid (pixel at 10 m resolution) is also shown. (For interpretation of the references to color in this figure legend, the reader is referred to the web version of this article.)

Table 5
Date of crop parameter field measurements.

Year	DOY	DAT	Date	LAI	MC-100	Field spec
2016	159	35	07/06	x		
	160	36	08/06		x	x
	174	50	22/06	x		
	175	51	23/06		x	x
	188	64	07/07	x		
	189	65	08/07		x	x
	209	85	27/07[a]	x		
2017	156	37	05/06	x	x	x
	174	55	23/06		x	x
	194	75	13/7		x	x
	214	95	2/8		x	x

DOY – Day of the year.
DAT – Day after transplanting.
LAI – Leaf area index.
MC-100 – Chlorophyll concentration meter instruments (Apogee Instruments, 2014).
Field Spec – Portable spectroradiometer instrument.
[a] For this date, due to the presence of cloud not Field Spec measurements neither Sentinel-2A image were available.

dhus/#/home); added value product can be obtained through the Sentinel Application Platform (SNAP), a software package tailored to the Sentinel-2 characteristics, developed by ESA (http://step.esa.int/main/toolboxes/sentinel-2-toolbox/sentinel-2-toolbox-features/). In particular the Sen2Cor algorithm (Müller-Wilm, n.d) process Level 1C data to an orthoimage Bottom of Atmosphere (BoA) corrected reflectance product (Level 2A), while the Biophysical Processor computes crop biophysical products (Level 2B) from Sentinel-2 reflectance data.

The technical characteristics of the MSI on-board the Sentinel-2 satellites are outlined in Table 2.

In the context of FATIMA project, the University of Natural Resources and Life Science (BOKU) has implemented for all the project study areas a data service platform for processing Sentinel-2 data (Vuolo et al., 2016). The service platform provides access to individual Sentinel-2 granules (ortho-rectified image tiles of $100 \times 100\,km^2$ in UTM/WGS84 projection) processed at level-2A (BoA) using the ESA Sen2Cor algorithm (Müller-Wilm, n.d). The platform also provide value-added products - obtained from the Sentinel Application Platform (SNAP) biophysical processor - with a focus on agricultural vegetation monitoring, such as LAI, and Fraction of vegetation Cover (F_{vc}: used in this study for the calculation of the R_n - net rainfall)., The improved spectral and spatial resolution of the Sentinel-2 satellite data allows the application of canopy radiative transfer models and computational efficient inversion techniques based e.g. on artificial neural network (ANN) to estimate crop biophysical parameters. In particular for LAI and F_{vc}, are obtained by an ANN algorithm trained using radiative transfer simulations from PROSPECT (Jacquemoud and Baret, 1990), and SAIL (Verhoef, 1984) models, and tailored for Sentinel-2 data. Detailed description of the algorithm can be found in Weiss and Baret, 2016. The algorithm requires eight Sentinel-2 spectral bands (B3-B7, B8a, B11 and B12) at 10 and 20 m pixel size, which are all resample to 10 m pixel size to derive LAI and F_{vc}. Experimental studies have shown the accuracy of this approach for LAI (Atzberger and Richter, 2012; Vuolo et al., 2016; Weiss and Baret, 2016) estimation in different environments and crops.

The broadband surface albedo is calculated as the integration of at-surface reflectance across the shortwave spectrum (D'Urso and Calera,

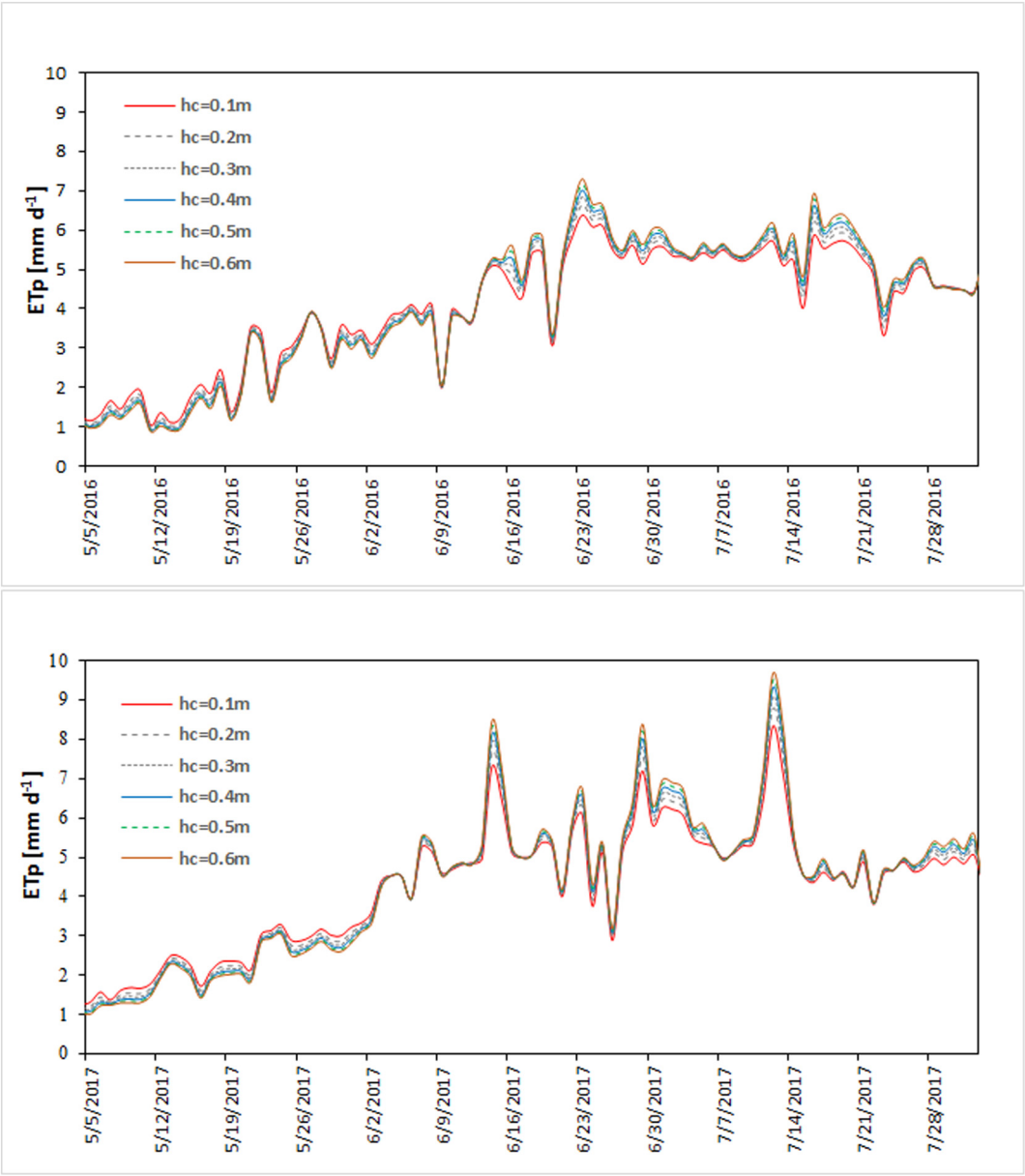

Fig. 5. Relationship between potential evapotranspiration (ET_p) and crop height (h_c) ranging from 0.1 and 0.6 m during season 2016 (top graph) and 2017 (bottom graph).

2006), as shown in equation (Eq. (1)).

$$\alpha = \sum_{bi} |\rho_{bi} \cdot \omega_{bi}| \quad (1)$$

where α is albedo, ρ_{bi} is surface reflectance for a given band b_i at Level-2A Sentinel-2A surface reflectance, obtained using the ESA's Sen2Cor algorithm (Version 2.3.1), ω_{bi} is the weighting coefficient representing the solar radiation fraction derived from the solar irradiance spectrum (Thuillier et al., 2003) within the spectral range (spectral response curves) for bands b_i (indicated with Esun in Table 3) and is calculated as equation (Eq. (2)):

$$\omega_{bi} = \frac{\int_{LO_{bi}}^{UP_{bi}} R_{s\lambda} \cdot d\lambda}{\int_{0.4}^{2.4} R_{s\lambda} \cdot d\lambda} \quad (2)$$

where $R_{s\lambda}$ is extra-terrestrial irradiance for wavelength λ (μm); and UP_{bi} and LO_{bi} are upper and lower wavelength bounds for Sentinel-2A band b_i, respectively.

Since 19th December 2017, a new version of the spectral response function is available (https://earth.esa.int/documents/247904/685211/S2-SRF_COPE-GSEG-EOPG-TN-15-0007_3.0.xlsx - accessed on 9th February 2018). The site provides an excel file with the spectral response functions. All the visible and near infrared bands have changed a little, even if only three bands have significant changes, B1, B2 and B8: B2 equivalent wavelength changes by 4 nm, B1 by 1 nm, and B8 by 2 nm. The SWIR bands did not change. Table 3 lists the bands settings for Sentinel-2A bands 1, 9, 10 (all not available after Sen2Cor processing), 8a (in the spectral range of band 8) and band 12 (negligible value for weighting coefficient) not taken into account for the albedo calculation.

This calculation procedure has been validated by BOKU through a comparison to ground measurements of albedo obtained with a Campbell CNR-1 radiometer installed at 2 m height from top of canopy, over a broad range of LAI values and vegetation classes (Vuolo et al., 2016).

Table 4 shows the temporal frequency of the Sentinel-2A (tiles 32TQM and 32TQN) cloud-free images, and derived products (α, LAI)

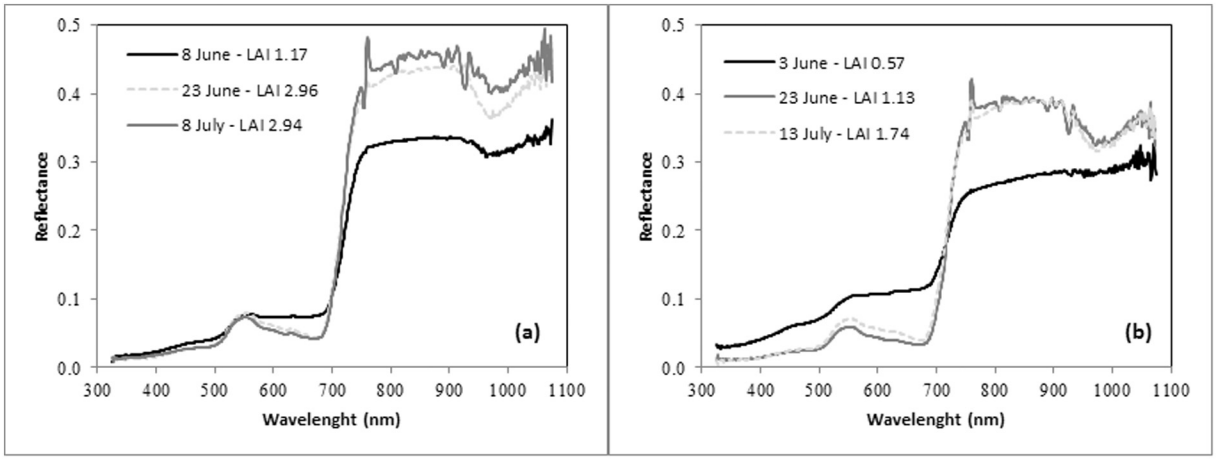

Fig. 6. Spectral variation of tomato reflectance curves for 2016 (a) and 2017 (b). In situ LAI (measurement taken on 7th and 22th June and 7th July) for 2016, and LAI from Sentinel-2A for 2017 are also reported.

which allowed to monitor the vegetation development throughout the 2016 and 2017 growing seasons.

3.3.3. In-situ crop and soil measurements

Crop and soil were characterized in selected geo-located positions during field campaigns carried in the experimental site at main phenological stages in the growing seasons 2016 and 2017. Crop measurements consisted of LAI, spectral reflectance and chlorophyll content, executed in 5 specific locations distributed along 4 transects of 60 m in each field (Fig. 4, green dots).

Measurements were taken in coincidence of Sentinel-2A acquisitions (Table 5).

The LAI was measured non-destructively by using a portable canopy digital analyzer (LAI-2000 Plant Canopy Analyzer, LI-COR), under conditions of diffuse illumination at sunset, in the day antecedent to the spectroradiometer measurements. The LAI value at each location is resulting as the average of 3 repetitions of 8 below canopy readings taken within a 5 m radius of the georeferenced location. An opaque cover (view cap) on the optical sensor, with an open wedge of 180°, was used to avoid the influence of neighboring obstacles, such as the operator (Gower and Norman, 1991; Li-Cor, 1992).

Canopy reflectance was measured by means of portable spectradiometer (ASD FieldSpec HH, Boulder, USA) operating in the wavelength range 325–1075 nm with 1 nm spectral resolution, controlled by a laptop equipped with the software provided by the instrument manufacturer. The instrument lens had a field of view of 25° and it was positioned at about 1 m above the canopy. All spectral readings were collected under clear sky conditions with no wind, between 9:30 and 11:30 local time (satellite overpass around 10:30 UTC), in correspondence of the same location of the LAI measurements. The measurement protocol included: collection of white reference on a calibrated Spectralon panel of dimensions 25 × 25 cm (SRT-99-100 Labsphere, Sutton, USA); collection of 3 sets of 10 reflectance spectra within 2 m from the reference location, which were successively averaged to reduce the signal/noise ratio of each measurements.

Soil water content was recorded continuously at 0.3 m depth in 5 points in the center of each pair of transect for the crop measurements (Fig. 4, blue dots), distant 15 m each other; in addition, at the center position of the transect a Profile probe PR 2/6 (Frequency Domain Reflectometry) giving readings at 10/20/30/40/60 and 100 cm (https://www.delta-t.co.uk/product/pr2/). All the probes of the same transect were connected to a GP2 datalogger (Delta T device, https://www.delta-t.co.uk/product/gp2/). Data from GP2, expressed as volumetric water content and °C, had been retrieved each other week on average during growing season. The soil water content readings were used for calibrating and validating the soil water balance in EPIC (see Section 3.4.2).

3.4. Methodology

3.4.1. Determination of crop evapotranspiration by Earth Observation-direct approach

The EO-direct approach for calculation of ET_p described in Section 2 is applied by using the crop parameters (α and LAI) derived from processing of Sentinel-2A data, assuming fixed values for the stomatal resistance ($sr \approx 100\ sm^{-1}$) and h_c (0.4 m), for the calculation of the aerodynamic resistance, in the case of herbaceous crop. The assumption of a constant h_c is consistent with the sensitivity analysis published by Consoli et al. (2006) – which report a value of 0.6 m for tree crops - and D'Urso (2010), considered valid for irrigated environments with the radiative component of the FAO-56PM equation dominant over the aerodynamic term. So doing, the calculation of ET_p requires standard meteorological data, LAI and surface α. To confirm the validity of this assumption a sensitivity analysis of the influence of fixed h_c (0.4 m) on ET_p was performed for the year 2016 and 2017 (Fig. 5).

The assumption of average constant value of $h_c = 0.4$ m determines an error percentage, ranging from −2% (as respect to the crop eight of 0.1 m) and 1% (as respect to the 0.6 m crop eight), on ETp cumulated value during irrigation seasons 2016 and 2017 (from May to August).

The IWR is then calculated by considering the following simplified equation (Eq. (3)):

$$IWR = ET_p - R_n \quad (3)$$

where R_n is net rainfall. Runoff and percolation are considered negligible considering the low amount of rainfall during the two growing seasons.

R_n was calculated in equation (Eq. (4)) as a function of the actual rainfall (R), LAI and Fractional Cover (F_{vc}) by using the semi-empirical model of interception proposed by Braden (1985).

$$R_n = R - a \cdot LAI \cdot \left(1 - \frac{1}{1 + \frac{F_{vc} \cdot R}{a \cdot LAI}}\right) \quad (4)$$

where R is the actual rainfall in ($mm\ d^{-1}$), and a in ($mm\ d^{-1}$) is an empirical parameter representing the crop saturation per unit foliage area (~0.28 for most crops).

3.4.2. Soil water balance and actual evapotranspiration computing using EPIC model and calibration procedure

Micrometeorological methods such eddy-covariance are often not

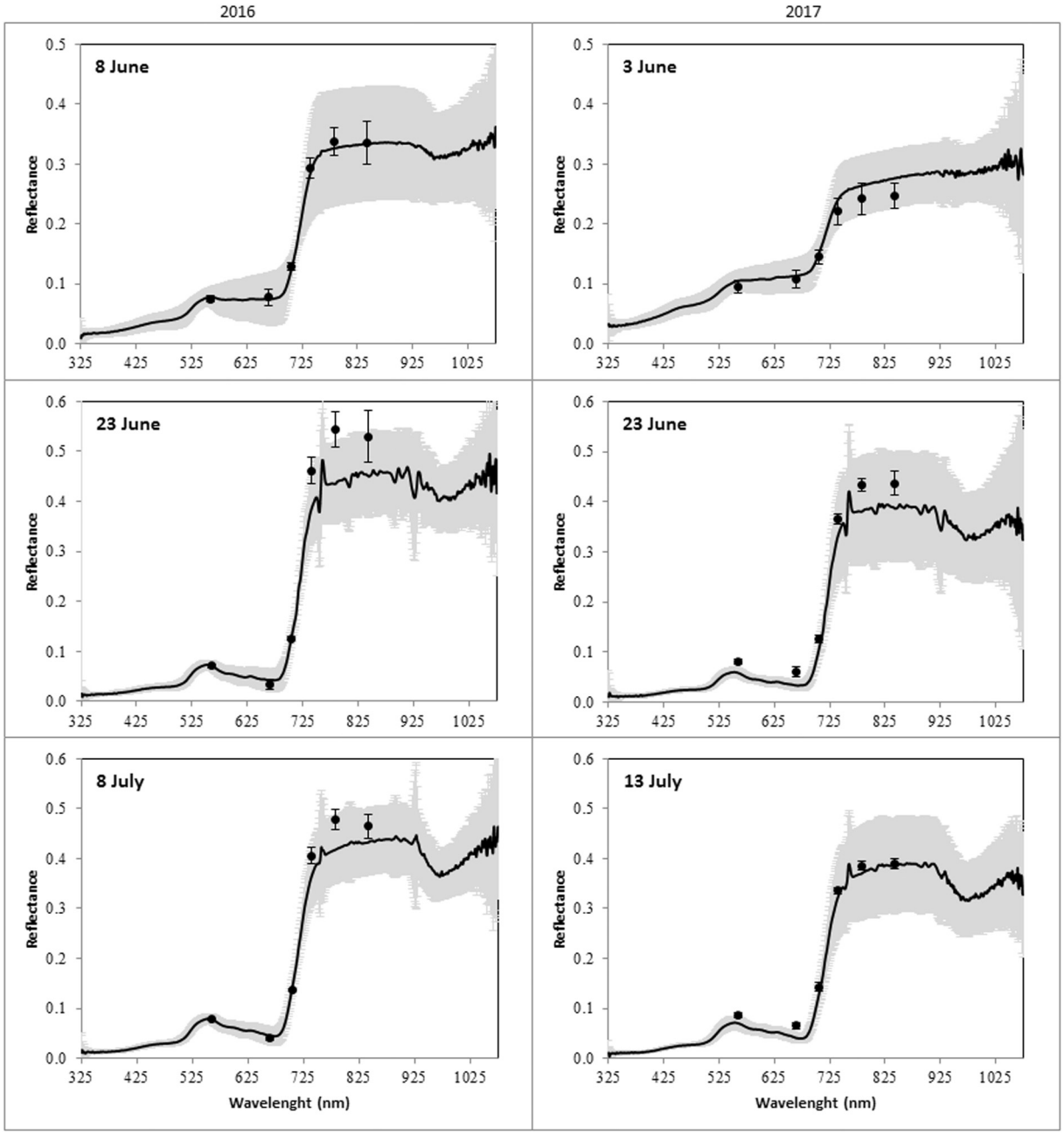

Fig. 7. Comparison between field spectral measurements (black line) and Sentinel-2A Bottom-of-Atmosphere (BoA) spectral reflectance (black circle point) for 2016 (left panel) and 2017 (right panel). Standard deviation for both Filed Spec (gray area) and Sentinel-2A (vertical bar) are also shown. The plots include only Sentinel-2A data in the spectral domain (350–1075 nm) corresponding to the Field Spec in-situ data.

Table 6
Statistical parameters for Leaf Area Index (LAI) values from field observation and Sentinel-2A product (n = 60).

LAI [m^2/m^2]	In-situ LAI-2000	Sentinel-2A - LAI by ANN
Minimum	0.61	0.81
Average	2.35	2.51
Median	1.77	2.77
Max	4.37	4.86
Range	3.76	4.05
Standard deviation	1.24	1.05

applicable in many conditions, due to their requirements in terms of crop uniformity and plot extension; these limits unfortunately occur very often in Mediterranean agricultural systems, due to high fragmentation and complex landscape. Hence, in order to validate the EO-based estimation of ET for the irrigated tomato and to verify the existence of the standard conditions underlying the PM direct approach, the soil water balance (SWB) was calculated using the EPIC biophysical model (Williams, 1995). EPIC successfully tested in many pedo-climatic situations (Farina et al., 2011) was selected for its capability of simulating daily crop growth and SWB. Mandatory inputs to run the model are: meteorological data, soil characteristics, crop growth data (i.e. plants density and crop growing period) and management (such as tillage, irrigation volumes and amount of fertilizers distributed). EPIC was calibrated using LAI (derived from field measurements and Sentinel-2A) and observed soil water content.

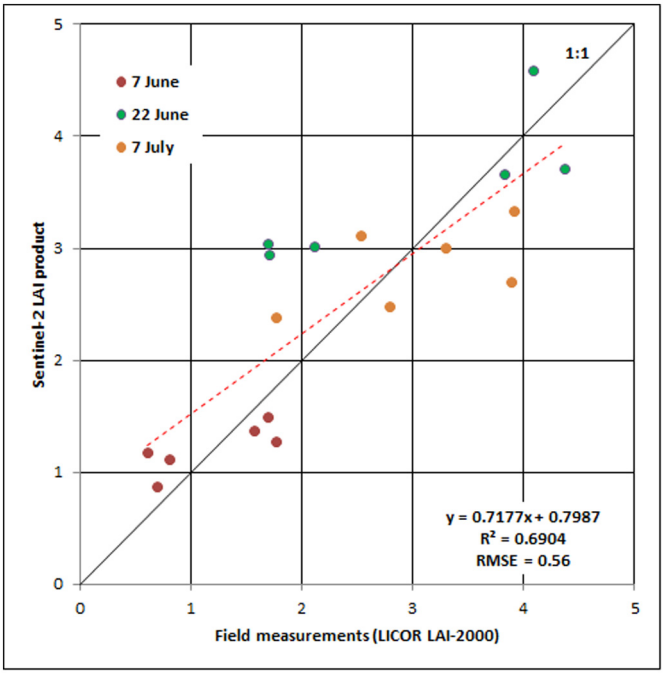

Fig. 8. Scatterplot (year 2016, n = 18) of field LAI measured vs. Sentinel-2A LAI product; reported dates are for field measurements while corresponding date of Sentinel-2A acquisition images are 8th and 23rd June, and 8th July.

SWB (mm) is estimated by the model as the difference between the water inputs (rainfall + irrigation) and outputs (runoff, percolation, and evapotranspiration) (Williams, 1995) at rooting depths, considering different layers. Actual rainfall and irrigation were input to the model. Runoff volume is estimated by the curve number technique (USDA, 1972). Water that does not run-off percolates and flows from the surface to the bottom layers, when soil water content exceeds Field Capacity. EPIC model offers several equations to calculate potential ET. Considering the experimental site conditions and data availability, the PM method was selected because it perform better in terms of crop growth and SWB. During calibration step, a set of sensitive model parameters at crop and soil level were selected and adjusted to maximize the agreement between model simulation and observations. For the variables affecting the crop growth, plant density and harvest index were input to the model according to the values measured in the field. Maximum LAI, the fraction of growing season when LAI declines, and the LAI decline rate were adjusted, in order to fit the estimated daily LAI output to data estimated by Sentinel-2A. At soil level, the value of the following parameters was modified respect to default values: root growth-soil strength (set to 1.5 to minimize stress on root growth), soil evaporation coefficient (set to 1.5 to better predict soil evaporation rate from top 20 cm soil depth) and the PM adjustment factor (set to 1 to better estimate PM-ET_p).

Table 7
Soil bulk density (g/cm^3), water content at Field Capacity (vol/vol) and at Wilting Point (vol/vol) for the top and subsoil of the soils in the 2016 and 2017 experimental trials.

Soil feature	Topsoil	Subsoil
2016 plot		
Bulk density	1.22	1.38
Field Capacity	27.2	32.8
Wilting Point	13.6	17.2
2017 plot		
Bulk density	1.25	1.37
Field Capacity	28.7	31.7
Wilting Point	14.1	14.7

3.4.3. Statistical analyses

Four types of metrics were calculated in order to assess the performance of the simulations:

1. the Root Mean Square Error (RMSE), a difference-based evaluation, giving an indication of the coincidence or lack of coincidence between simulated and measured value, was calculated. RMSE indicates the difference between measured and simulated values and has the advantage of producing a result in the same units as that used for measurement. The calculated RMSE can be compared with the size of difference that is considered acceptable;
2. the Pearsons's r coefficient of correlation that is a measure of the correlation between measured and predicted data. It assesses the linear relationship, i.e. values of one variable show a continuous increase or decrease as values increase or decrease on a second variable, even though the trend may not be linear. High values of the Pearson correlation coefficient suggest high predictability.
3. the linear regression R^2 was also used. In the regression between observed and model-estimated values estimates of the intercept and the slope are good indicators of accuracy. Best values of intercept and slope are zero and 1, respectively.
4. the Root Mean Square Difference (RMSD) was used in order to compare two estimates (as in the case of the two modelled estimates of ET, FAO-56 PM and EPIC), rather than comparing an estimate and measured value.

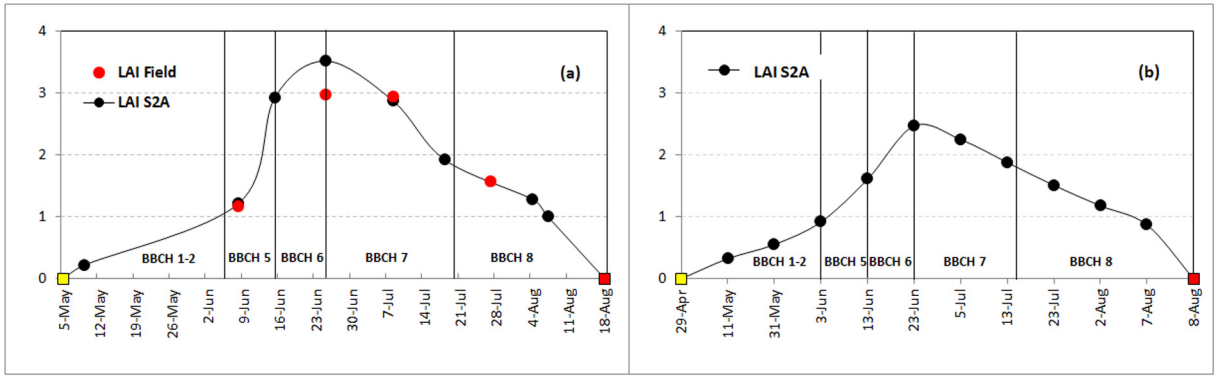

Fig. 9. Time evolution of Sentinel-2A LAI product for the growing seasons 2016 (a) and 2017 (b). For year 2016 average value of LAI from field measurements (included the date of July 27th where no Sentinel-2A images were available) are also plotted in the respective graph. (yellow square = transplanting date; red square = harvesting date). (For interpretation of the references to color in this figure legend, the reader is referred to the web version of this article.)

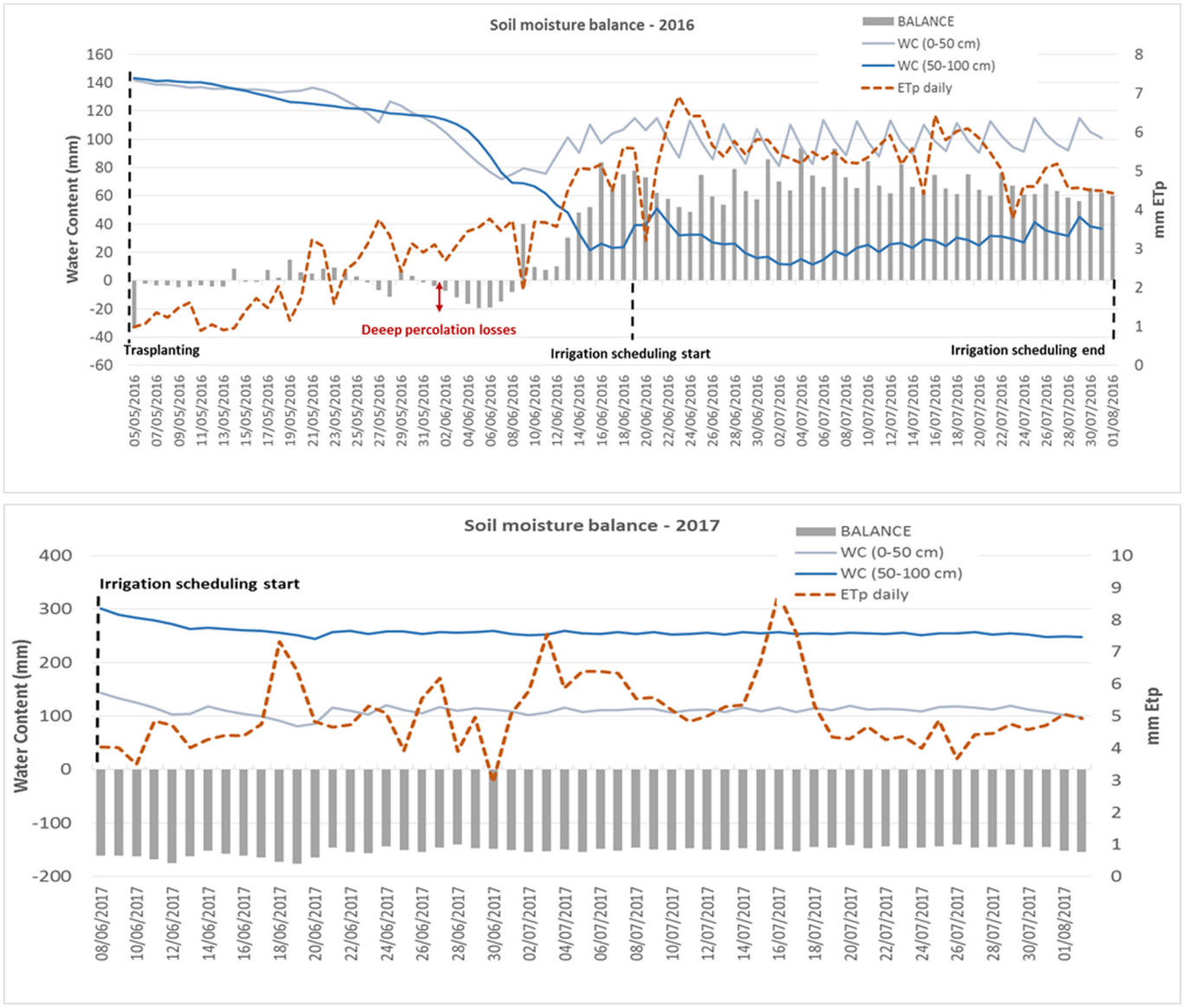

Fig. 10. Daily evolution of Soil Moisture balance (mm d^{-1}) represented with gray bars, calculated starting from Frequency Domain Reflectometry (FDR) measures in the 0–50 cm RSMZ (gray line), and in the 50–100 cm deep soil zone (blue line) for 2016 (top chart), and 2017 (bottom chart). With orange dotted line are showed also the daily ETp values (mm). (For interpretation of the references to color in this figure legend, the reader is referred to the web version of this article.)

Table 8
Water losses by deep percolation according to the irrigation volumes provided by the farmer for the 2016 and 2017 crop seasons.

Crop season	2016[a]	2017
Deep percolation (m^3/ha)	636	3049
Total irrigation (m^3/ha)	3340	6620
% of water losses on total irrigation	19	46

[a] Water losses were observed only during the first 5 May–8 June period (irrigation supply was applied in two times by sprinkler system).

4. Results and discussion

This section first focuses on the analysis of the spectral consistency of Sentinel-2A BoA reflectance data, and quality of Sentinel-2A data for the retrieval of LAI, compared with ground measurements. Then, it presents the inter-comparison of the EO-based ET_p with the ET_a derived from the SWB predicted by EPIC model.

4.1. Spectral data

To verify the spectral consistency of Sentinel-2A BoA reflectance data with ground reflectance measurements, in different atmospheric condition and illumination-viewing geometry of the sensors, we have used the spectroradiometer measurements reported in the Section 3.3.3.

Reflectance spectra of tomato canopy varied significantly during the growing season and between years. Fig. 6 presents the continuous spectra, from Field Spec, for the two-experimental campaigns, with the corresponding in-situ LAI for 2016 and LAI from Sentinel-2A for 2017.

At the beginning of the *inflorescence emergence* stage (beginning of June) and in correspondence of low LAI, the reflectance in the Red spectral region (maximum Chl absorption around 670 nm) is higher, while the NIR reflectance (from 785 to 900 nm) is lower. By the increasing of LAI, (in the mid-season second half of June until first decade of July - at the *flowering* stage) reflectance in the Red region decreases, conversely the NIR reflectance increases. The difference in the increase of reflectance in the red-edge (from 710 to 750 nm), i.e. the slope connecting the local minimum reflectance in the Red region, maximum

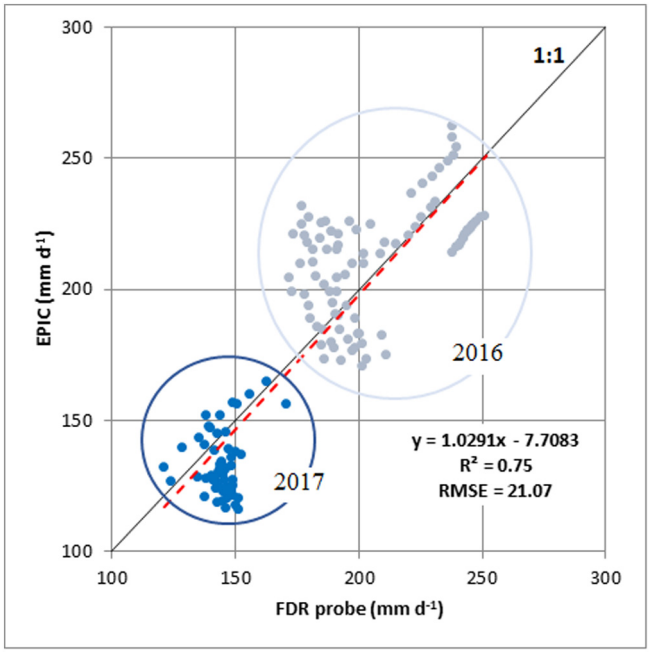

Fig. 11. Comparison between measured Frequency Domain Reflectometry (FDR) probe content (mm d^{-1}) and simulated (EPIC) Root Zone Soil Moisture (RZSM) content (mm d^{-1}), at 0–60 (2016 - from 6th May to 1st august n = 89) and 0–40 (2017 - from 6th June to 2nd August n = 56) cm soil depth.

Table 9
Statistical parameters for ET_p, and ET_a during the period from 5 May to 8 August for 2016 and 2017 growing seasons.

	ET_a	ET_p
2016		
Minimum	0.46	0.49
Average	3.30	3.32
Max	5.78	6.02
Range	5.51	5.53
Seasonal	314	315
2017		
Minimum	0.33	0.33
Average	3.53	3.66
Max	6.80	6.90
Range	6.47	6.57
Seasonal	336	348

absorption of chlorophyll, and the region with high reflectance values of the NIR plateau, affected by plant cell structure and leaf layers can be also clearly noticed.

The peaks around 760 nm for the acquisition of 23rd June 2016 and 23rd June 2017 were due to variability in the atmospheric water column which are generally smoothed in successive steps of the analysis.

In Fig. 7 the values of Sentinel-2A BoA reflectance are superimposed to the spectral measurements taken in coincidence of the satellite acquisition. The BoA values for the Sentinel-2A images are representing the average value for the portion of field where spectral measurement were taken (around 20 pixels at 10 m resolution) while the spectra represented are the average of all the measurements taken. A good agreement between Sentinel-2A signatures and the reflectance measured with the Field Spec was found, although differences can be noticed among different spectral bands and surface reflectance changes within the acquisition dates. Although the spectral variation, the crop reflectance curves maintain the same behavior in both years. Different value (in terms of reflectance units) can be observed between the two-years (lower in 2017 with respect to 2016). This can be ascribed to the climatic conditions in the two years, characterized by different seasonal rainfall and temperature patterns.

4.2. Leaf Area Index data

The quality assessment of the LAI derived from the Sentinel-2A was performed through comparison with non-destructive field reference measurements (LAI-2000 Plant Canopy Analyzer), described in Section 3.3.3. Table 6 reports the main statistical parameters for the 2016 field campaign related to LAI measured and satellite estimates.

The satellite estimations and the ground observations are significantly correlated with one another, $r = 0.83$, $p < 0.01$, with $R^2 = 0.69$, and RMSE of 0.56 m^2/m^2 (25% of the mean value), confirming the high potential and quality of Sentinel-2A data for the retrieval of LAI based on the full spectral information available (Herrmann et al., 2011; Vuolo et al., 2016). Fig. 8 shows the scatterplot (for three different date) of field and satellite LAI estimates of years 2016.

The time evolution of LAI - according to phenological stages from BBCH scale (Meier, 2001) - for the 2016 and 2017 growing seasons (from transplanting to harvest) is described in Fig. 9. In 2016 during the month of May at *leaves development* and *formation of side shoots* stage (BBCH 1-2) the LAI value was < 1 $m^2 m^{-2}$. From the first week of June at *inflorescence emergence* stage (BBCH 5) canopy progressively developed, reaching the maximum around the second half of June at *the flowering stage* (BBCH 6), with LAI values around 3.5 (Sentinel-2A) and 2.96 (field measurements) in 2016, and 2.47 in 2017. From this peak, during the *development of fruit* (BBCH 7) and *ripening of fruit and seed* in (BBCH 8) the LAI decreased down to the minimum before the harvest.

Due to the different meteorological trend characterized by different seasonal rainfall and temperature patterns, there is a clear decrease on the LAI in 2017 as respect to the 2016. This decrease confirms the importance of LAI on the crop productivity (Breda, 2003). In fact, there has been a large difference in yield in the two year, with 90.7 ton/ha (2016) and 72.3 ton/ha (2017), and this is clearly visible in the Sentinel-2A data confirming its potential to detect actual crop development conditions.

4.3. Soil Moisture, crop evapotranspiration and Irrigation Water Requirements

To evaluate the Soil Moisture balance, it was necessary to take into account some different physical and hydrological characteristics of the soils of the two experimental plots (2016 and 2017). Soil dry bulk density (BD), water content at Field Capacity (FC) and at Wilting Point (WP) measured at the beginning of each trial as average for the top and subsoils are reported in Table 7. These data were used to convert the moisture volumes measured with Frequency Domain Reflectometry (FDR) into mm of water present in the soil space (voids volumes).

The daily evolution of Soil Moisture content (mm d^{-1}) measured by Frequency Domain Reflectometry (FDR) probes, normalized in two depth ranges as the Root Zone Soil Moisture (RZSM) from 0 to 50 cm soil thickness, and the deep soil zone (not affected by most of the roots), from 50 to 100 cm of depth, are reported in Fig. 10 for the two years under investigation (2016 and 2017).

According to these two soil thicknesses, a simple daily balance was performed by considering also the Rain and the ET_p.

According to the Soil Moisture balance, as previous showed in Fig. 10, an overall estimation of the water losses due to deep percolation is reported in the following Table 8.

The Fig. 10 clearly shows as in the 2016 the water losses are concentrated in the first period of the crop season, form May to beginning of June. After this date the irrigation scheduling seems to be more efficient and the balance is always positive, as expression of the difference of moisture from RSZM to the deep soil zone. On the contrary, in the 2017, the soil moisture balance is always negative; the water

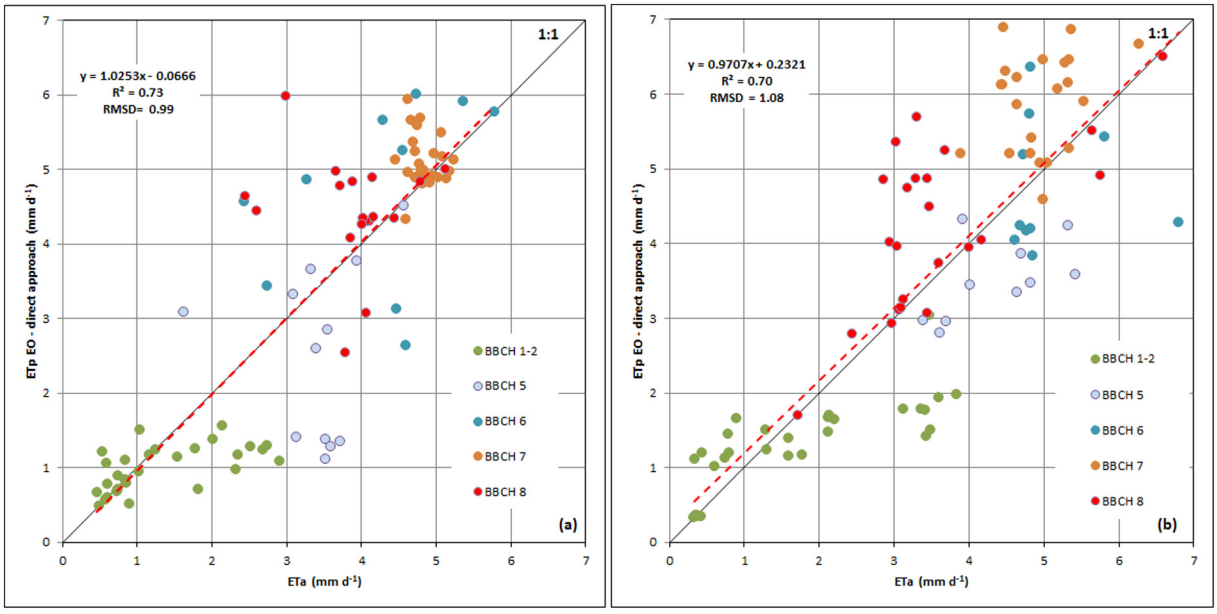

Fig. 12. Actual evapotranspiration (ET_a) vs. potential evapotranspiration (ET_p) estimated by EO direct approach from 5th May to 8th August at main phenological stages, in 2016 (a) and in 2017 (b) processing tomato growing season.

Table 10
Micro-irrigation applied in 2016 and 2017 growing season (volume in mm/ha).

2016												Total month
May	Day	5										**44**
	Volume	44[a]										
June	Day	9	13	16	19	20	22	25	28			**146**
	Volume	44[a]	15	15	15.6	15.6	15.6	12.5	12.5			
July	Day	1	4	7	10	13	16	19	22	26	30	**133**
	Volume	12.5	12.5	12.5	14.4	14.4	12.5	13.7	13.7	14.4	12.5	
August	Day	1	4	7								**41**
	Volume	13.7	13.1	14.3								
Total season												**364**

2017													Total month
May	Day	14	31										**88**
	Volume	44[a]	44[a]										
June	Day	8	13	20	23	26	29						**200**
	Volume	59.3	45.6	18.3	31.9	18.3	27.4						
July	Day	3	6	8	11	13	15	17	19	22	24	26	28	**347**
	Volume	32	22.8	41	32	32	27.4	36.5	32	23	18.3	18.3	32	
August	Day	2												**27**
	Volume	27												
Total season														**662**

Bold highlighted the total amount per month and season.
[a] Sprinkler irrigation. The amount of water applied with this irrigation system has been estimated based on the amount of water delivered of each plant (around 5 l) multiplied for the number of plants per ha (29.000).

amount given with the irrigation scheduling were always overestimated by the farmer, despite the ET_p trend (and consequently the IWR calculated by EO). These different trends are to be related to the different soil hydrological characteristics, topographic position (on fair slope or flat area) and also to the fixed irrigation scheduling adopted by the farmer.

To evaluate the effectiveness of the soil water balance, a further comparison between FDR measures and these predicted by the EPIC model was performed in the RZSM depth range, as reported below in Fig.11. Good agreement ($r = 0.86$, $R^2 = 0.75$, $p < 0.01$ and RMSE 21.07 mm d^{-1}) between simulated and measured soil water content in the root zone was observed.

With regards to the estimation of the daily ET_a, EPIC computes evaporation from soil and plant separately. Potential soil water evaporation is estimated as a function of potential evaporation and LAI using also exponential functions of soil depth and water content. For the plant evaporation the estimation is a linear function of potential evaporation and LAI.

Table 9 provides an overview of ET_p, and ET_a (EPIC) trends for the period from May 5th to August 8th for 2016 and 2017 growing seasons.

ET_a, derived from EPIC model, varied from 0.46 mm d^{-1} (May 20th) to 5.78 mm d^{-1} (June 25th) in 2016, and from 0.33 mm d^{-1} (7th May) to 6.80 mm d^{-1} (20th June) in 2017. The seasonal values of ET_a in the growing season ranged from 314 mm in 2016 to 336 mm in 2017.

ET_p varied from 0.49 (11th May) to 6.02 mm d^{-1} (23th June) in 2016, and from 0.33 (7th May) to 6.90 mm d^{-1} (2nd July) in 2017. The seasonal values of ET_p in the growing season ranged from 315 mm in 2016 to 348 mm in 2017.

Table 11
Comparison between water recorded data, and IWR estimate from EO-direct approach method during the two growing seasons.

Year	Month	Water meter	IWR
		Volume (mm/ha)	
2016	May	44	8
	June	146	103
	July	133	135
	August	41	26
	Total	364	272
2017	May	88	49
	June	200	117
	July	347	150
	August	27	22
	Total	662	338

A good agreement was found, $r = 0.85$ $p < 0.01$, $R^2 = 0.73$ for 2016, and $r = 0.83$ $p < 0.01$, $R^2 = 0.70$ for 2017, and RMSD of 0.99 and 1.08 mm $d^{-1}$for year 2016 and 2017 respectively, between tomato actual evapotranspiration (ET_a) derived from EPIC model, and ET_p estimated from EO-direct approach. The scatterplot in Fig. 12 shows the average daily value, for the main phenological stage, of ET aggregated at field scale (each point represents the average value of 20 measurements) derived from EPIC model (ET_a) and EO-direct approach (ET_p).

Irrigation was applied starting from transplanting and ended around one week before the harvest. The first irrigations were provided by sprinkler system, while for the rest of the season micro-irrigation was applied (Table 10).

Table 11 reports the irrigation volumes provided by the farmer, with micro-irrigation system, and the IWR derived by EO-direct approach in the same period.

To compare the evolution of IWR estimated by EO-direct approach and the actual irrigation applied by the farmer, daily value of IWR was

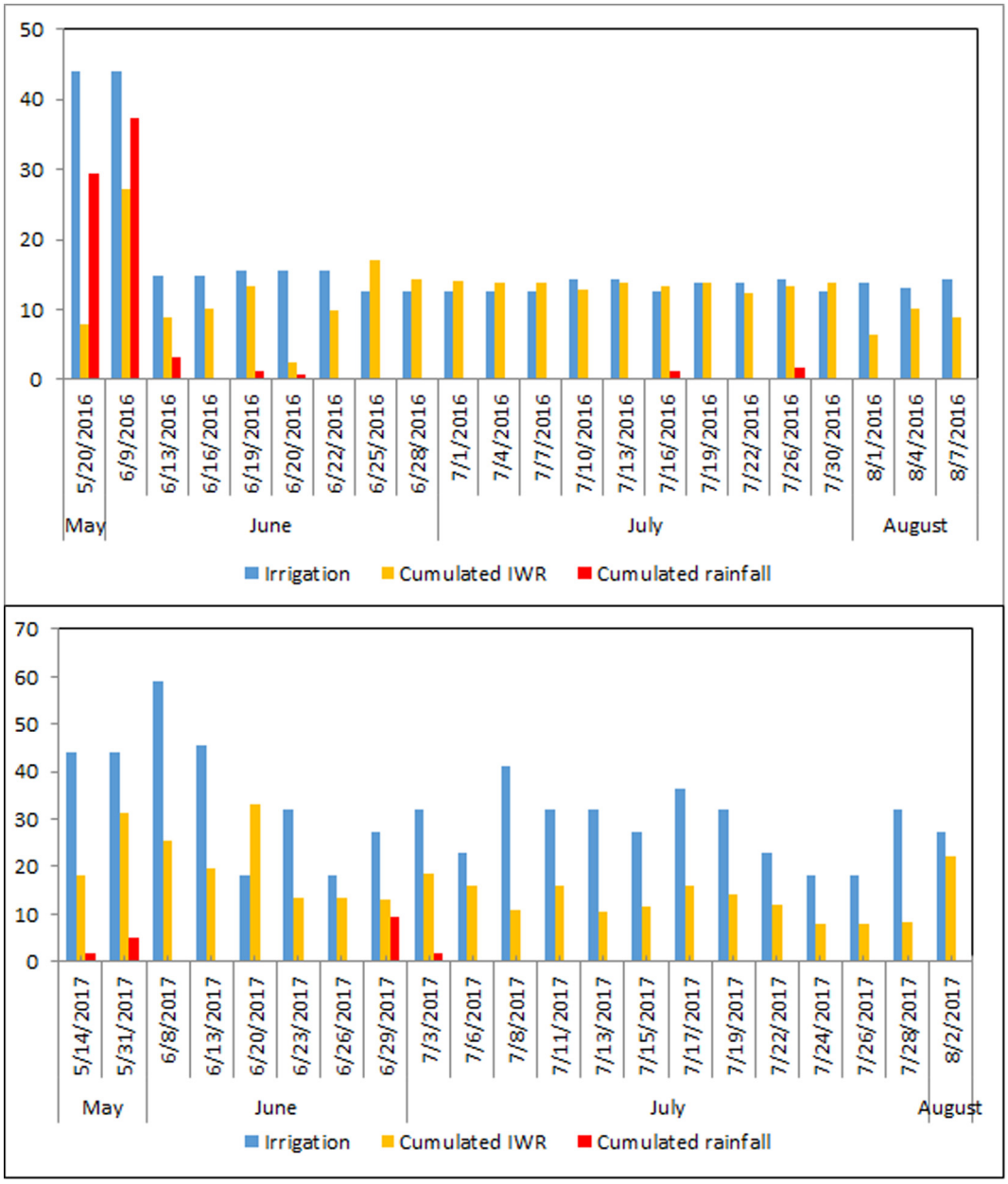

Fig. 13. Comparison between irrigation applied (mm) and accumulated IWR (mm) at same date, for year 2016 (top chart), and 2017 (bottom chart). Cumulated rainfall (mm) is also shown.

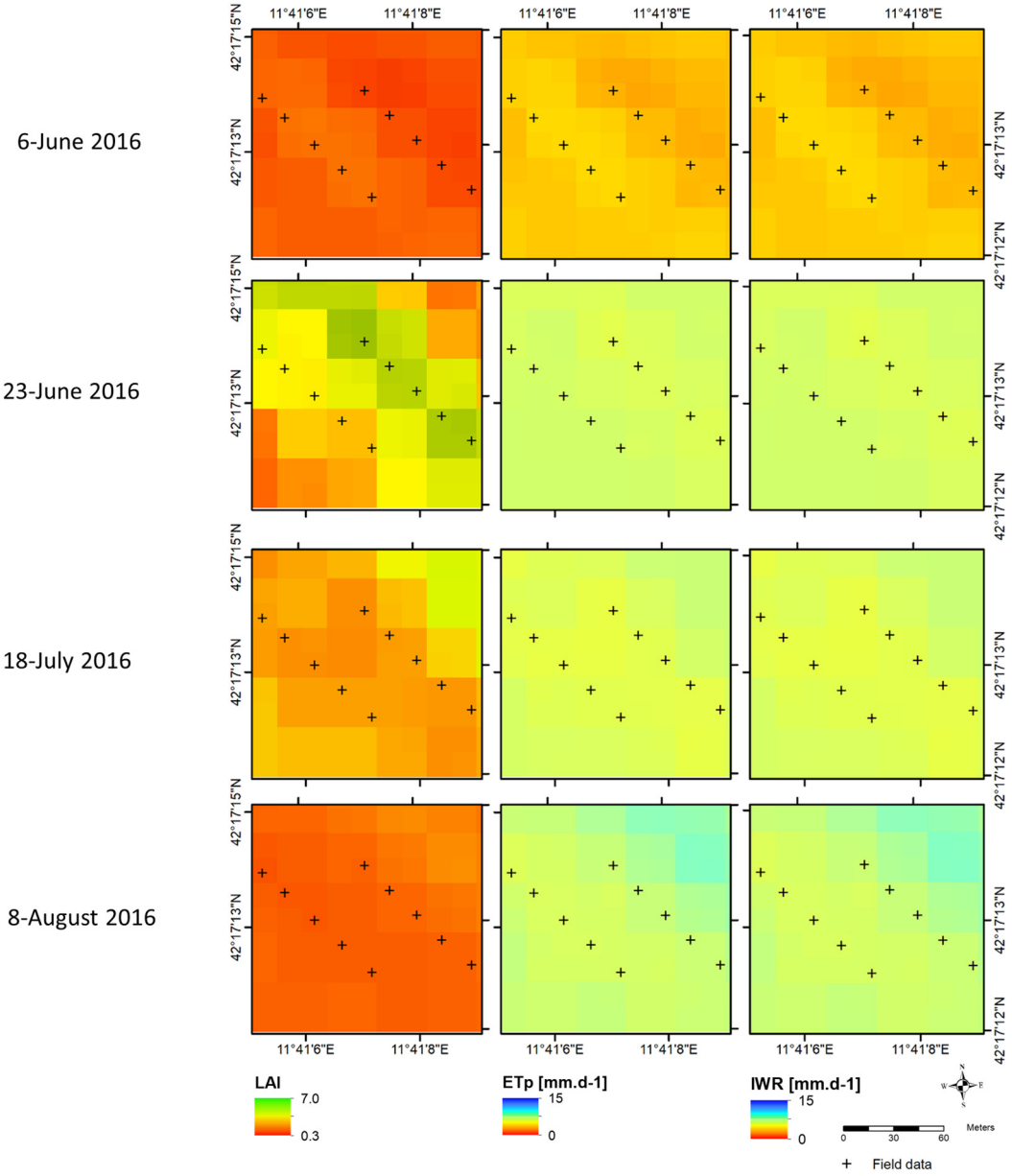

Fig. 14. An example of time-series maps of Leaf Area Index (LAI), potential evapotranspiration (ET_p) estimated by Earth Observation (EO) direct approach, and Irrigation Water Requirements (IWR) for the tomato study field.

accumulated at the same day of the irrigation as shown in Fig. 13.

The analysis of the data highlight that in both year the amount of water applied by the farmer is higher than satellite IWR estimates, although with differences between the two years (around +20% in 2016, and +50% in 2017). This discrepancy could be explained by considering the following factors:

- Lower precipitation (−75%) in 2017 compared to 2016
- Higher percolation rate, as shown in Fig. 10, below the root zone
- Soil characteristic together with the prolonged drought period favored the creation of very deep cracks, the increase of evaporation from cracks (from 12 to 30%) and the water loss from the root zone through percolation down to the bottom of cracks. Ritchie and Adams (1974) observed that cracks can increase evaporation by 12–30% (0.3 to 0.8 mm d^{-1}). Thus, the effect of cracks on water vapour movement and soil moisture evaporation is relatively important after a dry layer is formed at uncovered soil.

Those factors influenced the farmer behavior which, especially in situation of drought period tends to apply quantities of water that are considerably higher than the real needs of the crop, also considering that in this WUA the water allocation (and the application of corresponding fees) is done based on of the extension of irrigated area and not of water volumes. As a consequence, farmers are not motivated to adopt efficient water saving strategies, which results in generalized over-irrigation and misuses of water resources.

Fig. 14 shows the temporal evolution of the main parameters (LAI, ET_p and IWR) derived from this study for year 2016.

4.4. Web-GIS Satellite-based - IAS setting up

Some initiatives, implementing satellite-based irrigation advisory services, were developed and they proved to provide economic benefits creating advantages for the environment and opportunities for all of the users of water resources (Calera et al., 2017). Through these services the farmers and managers of water resources, evaluate the volume of

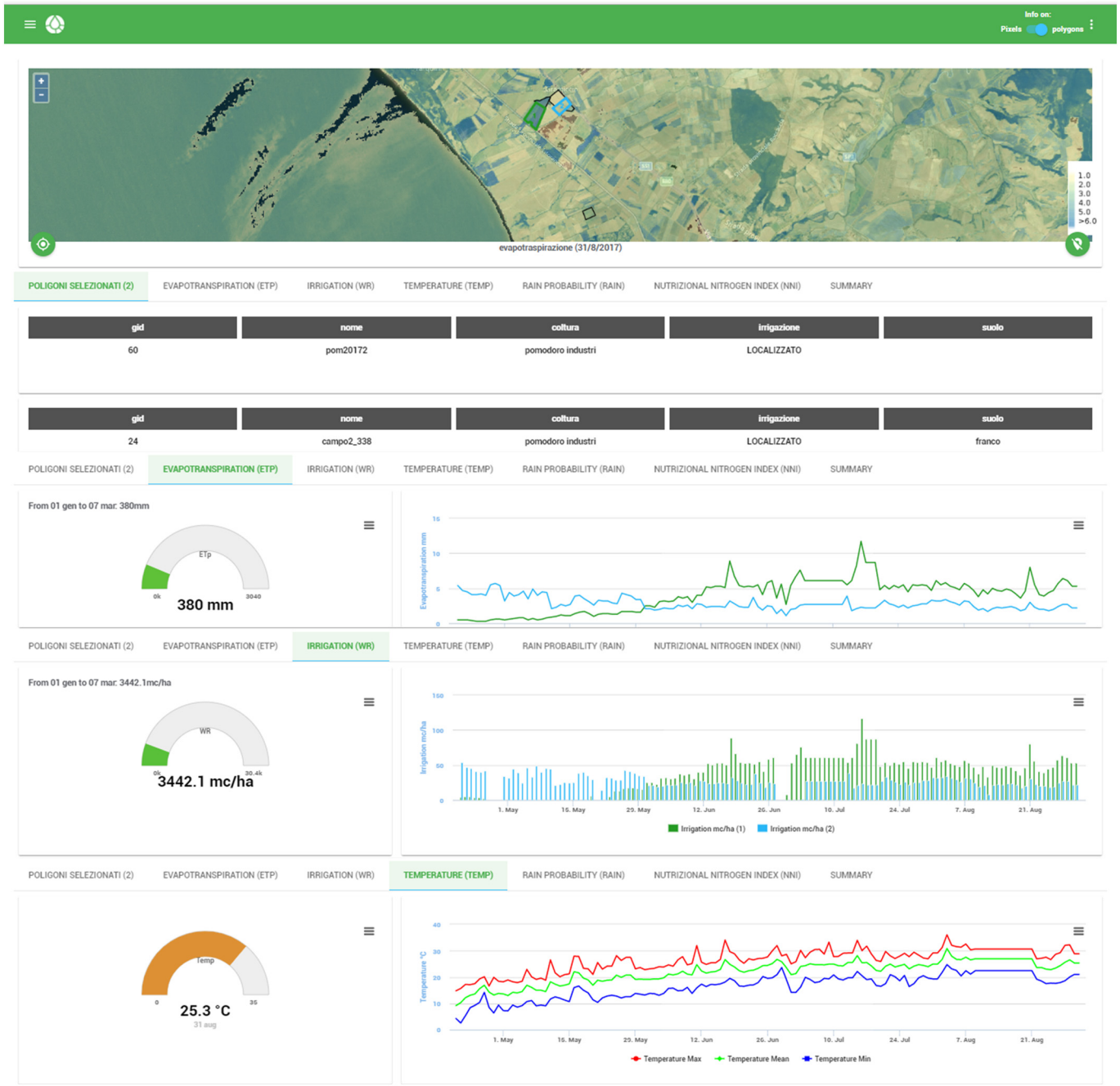

Fig. 15. IRRISAT: time series of ET_p, IWR and air temperature (minimum, average and maximum values).

irrigation water to be applied, get estimates of the growth and phenology of crops, and know the meteorological conditions in their area. For them, it means (i) a correct and economic scheduling of irrigation; (ii) a reduction of water and energy inputs; (iii) an optimization of work and production. In the FATIMA project, for the Italian pilot area two web-application have been developed: IRRISAT (http://fatima.irrisat.com/) (Fig. 15), dedicated to farmers and IRRISAT MTE (http://fatima.irrisat.com/italy/) (Fig. 16) dedicated to WUA. The maps and suggested irrigation volume applications are timely published on a dedicated web-based dashboard interface, with restricted access to farmers and water basin authorities, in order to better control the irrigation process and consequently improve its overall efficiency. An intuitive dashboard has been developed to give farmers the ability to monitor the canopy development, irrigation advice, evapotranspiration at plot level. Data as time series of LAI, ET_p beside other variables of potential interest (e.g. time series of IWR, rainfall, and air temperature) are shown in charts (Fig. 15). A similar interface was developed for the Irrigation Consortia and Water User associations. The tool allows the evaluation of crop water requirements aggregated at district level, for a more efficient management of the conveyance and distribution network. The GIS tools are going to be further expanded to link the financial management of the irrigation fees at farm level to the IWR (Fig. 16).

5. Summary and conclusion

This manuscript provides the descriptions of a methodology to estimate ET_p of processing tomato crop (*Solanum lycopersicum* L.) and the associated quantitative calibration of the remote sensing reflectance products derived from the MSI sensor on board Sentinel-2A, which are critical for the retrievals of ET constituents' parameters like LAI and α.

Fig. 16. IRRISAT Map Time Explorer (MTE): time series of NDVI, LAI, ET_P and IWR.

The main advances provided by our research activities is – thanks to the improved spectral/spatial and temporal resolution of the Sentinel-2 satellite – to provide a more physically-based methodologies (i.e. application of radiative transfer models), to detect the actual crop development and the estimate of the crop parameters (e.g. LAI) which influence the entity of evapotranspiration fluxes and hence the IWR, by using all the available spectral information, surpassing the traditional K_c approach based on tabulate data (coming from paper FAO-56), or on the linear relationship between Kc and VIs, which uses a limited numbers of spectral bands, and thus is not able to detect reflectance behavior of surface patterns with the same accuracy.

The results obtained confirmed the spectral consistency of Sentinel-2A data with ground reflectance measurements and the high potential and quality of Sentinel-2A data for the retrieval of LAI. Results indicate a good agreement between ET_p estimated by EO direct approach and the ET_a measured by means of a calibrated SWB. This approach confirms the validity of combining Penman-Monteith model with EO based vegetation parameters.

The results indicate that farmers tend to over-irrigate the crop. This behavior can mainly ascribed to the following factor:

- unavailability of supporting information about climate and canopy development, and
- in most cases, even in presence of metered distribution networks, the water allocation (and the application of corresponding fees) is done on the basis of the extension of irrigated area and not of water volumes. As a consequence, farmers are not motivated to adopt efficient water saving strategies, which results in generalized over-

irrigation and misuses of water resources.

In this context the availability of reliable, objective and timely information about the actual development of crop (and hence its Irrigation Water Requirements) allows the implementations of efficient water distribution criteria based on the actual irrigation needs of crops. The enhanced capabilities provided by ESA Sentinel-2 (A and B) mission, with global coverage at 10 days revisit frequency of each single satellite (5 days combined constellation) and 10–20 m spatial resolutions, are particularly suitable for mapping crops and irrigated areas, and related IWR, with satisfactory accuracy and in a cost-effective way, also considering the opportunities for combining the data with that from complementary systems, such as Landsat-8, to obtain cloud free dense time series over large geographic regions.

The availability of this unprecedented multi-spectral observations combined with the impressive.

progresses in the field of Information and Communication Technologies can facilitate the improvement/development of IAS using EO data as an operational service for supporting irrigation water management. Hence, nowadays satellite images are delivered via Internet within few hours from the acquisition time, and they can be quickly processed to get final-users products distributed in near-real time.

The services can provide to farmers and water resource manager sounder quantitative information about the spatial/temporal variability of crop growth conditions and its related IWR, improving crop production efficiency and reducing its environmental impact.

This information would be helpful to achieve the commitment to the increasingly stringent regulatory requirements (e.g. the EU Water Framework Directive 2000/60, water metering and full cost recovery, and the Rural Development Program 2014–2020, Ex-ante conditionalities on Water Resources), which imposes a substantial increase in the efficiency of water use in agriculture for the next decades from farmers and irrigation managers.

Acknowledgments

This research was developed in the framework of the project FATIMA (FArming Tools for external nutrient Inputs and water MAnagement), funded by the European Union's Horizon 2020 research and innovation programme (Grant Agreement No 633945). Special thanks are dedicated to the farmer Mr. Vincenzo Fava for making his land available for experimental set-up and data collection.

Author contributions

Pasquale Nino and Silvia Vanino led the conception, design and the writing/reviewing of the manuscript, participated to field measurements and to data analyses; Claudia Di Bene participated to field measurements and to data analyses, calibrated and run the EPIC model, and contributed to the writing/reviewing of the manuscript, Roberta Farina contributed to calibrate and run the EPIC model and participated to the writing; Bruno Pennelli set-up the experimental equipment, collected and analyzed the soil moisture content data and contributed to the manuscript revision; Salvatore Falanga Bolognesi performed Sentinel-2A image processing to compute ETp and IWR from EO-direct approach method; Francesco Vuolo provided BoA Sentinel-2A images and related value-added products; Guido D'Urso, Carlo De Michele and Rosario Napoli contributed equally to experimental set-up, systems analyses and the writing; Giuseppe Pulighe revised the manuscript and contributed to the writing and manuscript revision.

Conflicts of interest

The authors declare no conflict of interest.

References

Allen, R.G., Pereira, L.S., Raes, D., Smith, M., 1998. Crop evapotranspiration - guidelines for computing crop water requirements, irrigation and drainage, FAO Irrigation and drainage paper 56. Available from: http://www.fao.org/docrep/X0490E/X0490E00.htm, Accessed date: 1 December 2018.

Allen, R.G., Tasumi, M., Trezza, R., 2007. Satellite-based energy balance for mapping evapotranspiration with internalized calibration (METRIC) – model. J. Irrig. Drain. 133, 380–394. http://dx.doi.org/10.1061/(ASCE)0733-9437(2007)133:4(380).

Allen, M.R., Frame, D.J., Huntingford, C., Jones, C.D., Lowe, J.A., Meinshausen, M., Meinshausen, N., 2009. Warming caused by cumulative carbon emissions towards the trillionth tonne. Nature 458, 1163–1166. http://dx.doi.org/10.1038/nature08019.

Allen, R.G., Pereira, L.S., Howell, T.A., Jensen, M.E., 2011. Evapotranspiration information reporting: I. Factors governing measurement accuracy. Agric. Water Manag. 98 (6), 899–920. http://dx.doi.org/10.1016/j.agwat.2010.12.015.

Anderson, M.C., Allen, R.G., Morse, A., Kustas, W.P., 2012. Use of Landsat thermal imagery in monitoring evapotranspiration and managing water resources. Remote Sens. Environ. 122, 50–65. http://dx.doi.org/10.1016/j.rse.2011.08.025.

Apogee Instruments, 2014. Chlorophyll concentration meter model MC-100 - owner's manual. Available from: https://www.apogeeinstruments.com/content/MC-100-manual.pdf, Accessed date: 1 December 2018 (20 pp.).

Atzberger, C., Richter, K., 2012. Spatially constrained inversion of radiative transfer models for improved LAI mapping from future sentinel-2. Remote Sens. Environ. 120, 208–218. http://dx.doi.org/10.1016/j.rse.2011.10.035.

Avramova, V., Nagel, K.A., Abdelgawad, H., Bustos, D., Duplessis, M., Fiorani, F., Beemster, G.T.S., 2016. Screening for drought tolerance of maize hybrids by multi-scale analysis of root and shoot traits at the seedling stage. J. Exp. Bot. 67, 2453–2466. http://dx.doi.org/10.1093/jxb/erw055.

Bastiaanssen, W.G.M., Menenti, M., Feddes, R.A., Holstlag, A.A.M., 1998. A remote sensing surface energy balance algorithm for land (SEBAL). 1. Formulation. J. Hydrometeorol. 212–213, 213–229. http://dx.doi.org/10.1016/S0022-1694(98)00253-4.

Bisquert, M., Sánchez, J.M., López-Urrea, R., Caselles, V., 2016. Estimating high resolution evapotranspiration from disaggregated thermal images. Remote Sens. Environ. 187, 423–433. http://dx.doi.org/10.1016/j.rse.2016.10.049.

Braden, H., 1985. Ein Energiehaushalts- und Verdunstungsmodell für Wasser- und Stoffhaushaltsuntersuchungen landwirtschaftlich genutzter Einzugsgebiete (in German, An energy management and evaporation model for water and substance balance studies of agricultural use catchments). Mitteilungen Dtsch. Bodenkundliche Gesselschaft 42.S, 294–299.

Breda, N.J.J., 2003. Ground-based measurements of leaf area index: a review of methods, instruments and current controversies. J. Exp. Bot. 54 (392), 2403–2417 (in biblio).

Calera, A., Campos, I., Osann, A., D'Urso, G., Menenti, M., 2017. Remote sensing for crop water management: from ET modelling to services for the end users. Sensors 17, 1104. http://dx.doi.org/10.3390/s17051104.

Consoli, S., D'Urso, G., Toscano, A., 2006. Remote sensing to estimate ET-fluxes and the performance of an irrigation district in southern Italy. Agric. Water Manag. 81, 295–314. http://dx.doi.org/10.1016/j.agwat.2005.04.008.

Drusch, M., Del Bello, U., Carlier, S., Colin, O., Fernandez, V., Gascon, F., Hoersch, B., Isola, C., Laberinti, P., Martimort, P., Meygret, A., Spoto, F., Sy, O., Marchese, F., Bargellini, P., 2012. Sentinel-2: ESA's optical high-resolution mission for GMES operational services. Remote Sens. Environ. 120, 25–36. http://dx.doi.org/10.1016/j.rse.2011.11.026.

D'Urso, G., 2001. Simulation and Management of On-demand Irrigation Systems: A Combined Agrohydrological and Remote Sensing Approach. Wageningen Agricultural University (PhD Thesis). Available from: http://edepot.wur.nl/196807, Accessed date: 1 December 2018 (194 pp.).

D'Urso, G., 2010. Current status and perspectives for the estimation of crop water requirements from earth observation. Ital. J. Agron. 5, 107–120.

D'Urso, G., Calera, A., 2006. Operative approaches to determine crop water requirements from earth observation data: methodologies and applications. AIP Conf. Proc. 852, 14–25. http://dx.doi.org/10.1063/1.2349323.

D'Urso, G., D'Antonio, A., Vuolo, F., De Michele, C., 2008. The irrigation advisory plan of Campania region: from research to operational support for the water directive in agriculture. In: Santini, A. (Ed.), Irrigation in Mediterranean Agriculture: Challenges and Innovation for the Next Decades. In: Lamaddalena, N., Severino, G., Palladino, M. (Eds.), 2008. Options Méditerranéennes: Série A. Séminaires Méditerranéens, vol. 84. CIHEAM, Bari, pp. 25–31. Available from: http://om.ciheam.org/article.php?IDPDF=800946, Accessed date: 1 December 2018.

Falloon, P., Betts, R., 2010. Climate impacts on European agriculture and water management in the context of adaptation and mitigation - the importance of an integrated approach. Sci. Total Environ. 408, 5667–5687. http://dx.doi.org/10.1016/j.scitotenv.2009.05.002.

Farg, E., Arafat, S.M., Abd El-Wahed, M.S., El-Gindy, A.M., 2012. Estimation of evapotranspiration ETc and crop coefficient Kc of wheat, in South Nile Delta of Egypt using integrated FAO-56 approach and remote sensing data. Egypt. J. Remote Sens. Space Sci. 15, 83–89. http://dx.doi.org/10.1016/j.ejrs.2012.02.001.

Farina, R., Seddaiu, G., Orsini, R., Steglich, E., Roggero, P.P., Francaviglia, R., 2011. Soil carbon dynamics and crop productivity as influenced by climate change in a rainfed cereal system under contrasting tillage using EPIC. Soil Tillage Res. 112, 36–46.

Glenn, E.P., Neale, C.M.U., Hunsaker, D.J., Nagler, P.L., 2011. Vegetation index-based crop coefficients to estimate evapotranspiration by remote sensing in agricultural and natural ecosystems. Hydrol. Process. 25, 4050–4062. http://dx.doi.org/10.1002/hyp.8392.

Gower, S.T., Norman, J.M., 1991. Rapid estimation of Leaf Area Index in conifer and

broad-leaf plantations. Ecology 72, 1896–1900. http://dx.doi.org/10.2307/1940988.
Herrmann, I., Pimstein, A., Karnieli, A., Cohen, Y., Alchanatis, Bonfil, D.J., 2011. LAI assessment of wheat and potato crops by VENμS and Sentinel-2 bands. Remote Sens. Environ. 115, 2141–2151. http://dx.doi.org/10.1016/j.rse.2011.04.018.
Huete, A.R., 1988. A soil-adjusted vegetation index (SAVI). Remote Sens. Environ. 25, 295–309. http://dx.doi.org/10.1016/0034-4257(88)90106-X.
IPCC, 2013. In: Stocker, T.F., Qin, D., Plattner, G.-K., Tignor, M., Allen, S.K., Boschung, J., Nauels, A., Xia, Y. (Eds.), Climate Change 2013: The Physical Science Basis Working Group I Contribution to the Fifth Assessment Report of the Intergovernmental Panel on Climate Change. Cambridge University Press, Cambridge, United Kingdom and New York, NY, USA.
IUSS Working Group WRB (World Reference Base for Soil Resources), 2015. World Reference Base for Soil Resources 2014, update 2015 International soil classification system for naming soils and creating legends for soil maps. In: World Soil Resources Reports No. 106. FAO, Rome Available from: http://www.fao.org/3/a-i3794e.pdf, Accessed date: 1 December 2018 (203 pp.).
Jacquemoud, S., Baret, F., 1990. PROSPECT: a model of leaf optical properties spectra. Remote Sens. Environ. 34, 75–91. http://dx.doi.org/10.1016/0034-4257(90)90100-Z.
Kaley, H., Ben, A., Clunie, K., Silvia, N., Anne, M., Kamila, P., Martin, N., Julia, Z., 2017. Research for agri committee - the consequences of climate change for eu agriculture. follow-up to the COP21 - un paris climate change conference. European Parliament, directorate-general for internal policies. Available from: http://www.europarl.europa.eu/RegData/etudes/STUD/2017/585914/IPOL_STU(2017)585914_EN.pdf, Accessed date: 1 December 2018.
Kalma, J.D., McVicar, T.R., McCabe, M.F., 2008. Estimating land surface evaporation: a review of methods using remotely sensed surface temperature data. Surv. Geophys. 29 (4–5), 421–469. http://dx.doi.org/10.1007/s10712-008-9037-z.
Kustas, W.P., Anderson, M.C., Semmens, K.A., Alfieri, J.G., Gao, F., Hain, C.R., Cammalleri, C., 2016. A thermal-based remote sensing modelling system for estimating crop water use and stress from field to regional scales. Acta Hortic. 1112, 71–80. http://dx.doi.org/10.17660/ActaHortic.2016.1112.10.
Lal, R., Stewart, B.A., 2016. Soil-specific Farming: Precision Agriculture. CRC Press Taylor & Francis Group, Boca Raton London, New York (431 pp., ISBN 9781482245332).
Laurent, V.C.E., Schaepman, M.E., Verhoef, W., Weyermann, J., Chávez, R.O., 2014. Bayesian object-based estimation of LAI and chlorophyll from a simulated sentinel-2 top-of-atmosphere radiance image. Remote Sens. Environ. 140, 318–329. http://dx.doi.org/10.1016/j.rse.2013.09.005.
Liaghat, S., Balasundram, S.K., 2010. A review: the role of remote sensing in precision agriculture. Am. J. Agric. Biol. Sci. 5 (1), 50–55. http://dx.doi.org/10.3844/ajabssp.2010.50.55.
Li-Cor, 1992. LAI-2000 Plant Canopy Analyser: Instruction Manual. Nebraska Li-Cor, Inc., Lincoln (179 pp.).
McKersie, B., 2015. Planning for food security in a changing climate. J. Exp. Bot. 66, 3435–3450. http://dx.doi.org/10.1093/jxb/eru547.
Meier, U., 2001. BBCH-monograph. Growth Stages of Mono and Dicotyledonous Plants. Federal Biological Research Centre for Agriculture and Forestry, Blackwell, Berlin; Wien Available from: http://www.reterurale.it/downloads/BBCH_engl_2001.pdf, Accessed date: 1 December 2018 (158 pp.).
Mekonnen, M.M., Hoekstra, A.Y., 2016. Four billion people facing severe water scarcity. Sci. Adv. 2, e1500323. http://dx.doi.org/10.1126/sciadv.1500323.
Moore, F.C., Lobell, D.B., 2014. Adaptation potential of European agriculture in response to climate change. Nat. Clim. Chang. 4, 610–614. http://dx.doi.org/10.1038/nclimate2228.
Moran, M.S., Inoue, Y., Barnes, E.M., 1997. Opportunities and limitations for image-based remote sensing in precision crop management. Remote Sens. Environ. 61, 319–346. http://dx.doi.org/10.1016/S0034-4257(97)00045-X.
Mulla, D.J., 2013. Twenty-five years of remote sensing in precision agriculture: key advances and remaining knowledge gaps. Biosyst. Eng. 114, 358–371. http://dx.doi.org/10.1016/j.biosystemseng.2012.08.009.
Müller-Wilm, U. Sen2Cor software release note. Available online: http://step.esa.int/thirdparties/sen2cor/2.3.1/[L2A-SRN]%20S2-PDGS-MPC-L2A-SRN%20[2.3.1].pdf, Accessed date: 9 February 2018.
Neale, C., Bausch, W., Heerman, D., 1989. Development of reflectance-based crop coefficients for corn. Trans. ASAE 32, 1891–1899. http://dx.doi.org/10.13031/2013.31240.
Pereira, L.S., 2017. Water, agriculture and food: challenges and issues. Water Resour. Manag. 31, 2985–2999. http://dx.doi.org/10.1007/s11269-017-1664-z.
Richter, K., Hank, T.B., Vuolo, F., Mauser, W., D'Urso, G., 2012. Optimal exploitation of the sentinel-2 spectral capabilities for crop leaf area index mapping. Remote Sens. 4, 561–582. http://dx.doi.org/10.3390/rs4030561.
Ritchie, J.T., Adams, J.E., 1974. Field measurement of evaporation on from shrinkage cracks. Soil Sci. Soc. Am. Proc. 38, 131–134.
Thuillier, G., Hersé, M., Labs, D., Foujols, T., Peetermans, W., Gillotay, D., Mandel, H., 2003. The solar spectral irradiance from 200 to 2400 nm as measured by the SOLSPEC spectrometer from the ATLAS and EURECA missions. Sol. Phys. 214 (1), 1–22. http://dx.doi.org/10.1023/A:1024048429145.
Tucker, C.J., Elgin, H.J.-Jr., McMurtrey, J.E.I., Fran, C.J., 1979. Monitoring corn and soybean crop development with hand-held radiometer spectral data. Remote Sens. Environ. 8, 237–248. http://dx.doi.org/10.1016/0034-4257(79)90004-X.
USDA - Soil Conservation Service, 1972. National Engineering Handbook, Section 4, Hydrology. - Chapter 21, Design Hydrographs. U.S. Department of Agriculture, Washington D.C., U.S.A. Available from: https://directives.sc.egov.usda.gov/OpenNonWebContent.aspx?content=18393.wba, Accessed date: 16 March 2018 (127 pp.).
Vanino, S., Pulighe, G., Nino, P., De Michele, C., Bolognesi, S., D'Urso, G., 2015. Estimation of evapotranspiration and crop coefficients of tendone vineyards using multi-sensor remote sensing data in a mediterranean environment. Remote Sens. 7, 14708–14730. http://dx.doi.org/10.3390/rs71114708.
Verhoef, W., 1984. Light scaterring by leaf layers with appliocation to canopy reflectance modelling. The SAIL model. Remote Sens. Environ. 16, 125–141. http://dx.doi.org/10.1016/0034-4257(84)90057-9.
Verrelst, J., Rivera, J.P., Veroustraete, F., Muñoz-Marí, J., Clevers, J.G.P.W., Camps-Valls, G., Moreno, J., 2015. Experimental Sentinel-2 LAI estimation using parametric, non-parametric and physical retrieval methods - a comparison. ISPRS J. Photogramm. Remote Sens. 108, 260–272. http://dx.doi.org/10.1016/j.isprsjprs.2015.04.013.
Vuolo, F., D'Urso, G., De Michele, C., Bianchi, B., Cutting, M., 2015. Satellite-based irrigation advisory services: a common tool for different experiences from Europe to Australia. Agric. Water Manag. 147, 82–95. http://dx.doi.org/10.1016/j.agwat.2014.08.004.
Vuolo, F., Żółtak, M., Pipitone, C., Zappa, L., Wenng, H., Immitzer, M., Weiss, M., Baret, F., Atzberger, C., 2016. Data service platform for sentinel-2 surface reflectance and value-added products: system use and examples. Remote Sens. 8, 938. http://dx.doi.org/10.3390/rs8110938.
Weiss, M., Baret, F., 2016. S2 ToolBox level 2 products: LAI, FAPAR, FCOVER version 1.1. Available from: http://step.esa.int/docs/extra/ATBD_S2ToolBox_L2B_V1.1.pdf, Accessed date: 1 December 2018 (53 pp.).
Williams, J.R., 1995. The EPIC model. In: Singh, V.P. (Ed.), Computer Models of Watershed Hydrology. Water Res Publ, Littleton, CO, pp. 909–1000.
WWAP (United Nations World Water Assessment Programme), 2015. The United Nations World Water Development Report 2015: Water for a Sustainable World. UNESCO, Paris Available from: http://unesdoc.unesco.org/images/0023/002318/231823E.pdf, Accessed date: 1 December 2018.
Zarco-Tejada, P.J., Hubbard, N., Loudjani, P., 2014. Precision agriculture: an opportunity for EU farmers — potential support with the CAP 2014–2020. In: Joint Research Centre (JRC) of the European Commission, Available from: http://www.europarl.europa.eu/RegData/etudes/note/join/2014/529049/IPOL-AGRI_NT%282014%29529049_EN.pdf, Accessed date: 1 December 2018 (56 pp.).